JOURNAL OF GEOPHYSICAL RESEARCH, VOL. 90, NO. B12, PAGES 10,373-10,392, OCTOBER 10, 1985

GEOCHEMICAL AND SEDIMENTOLOGICAL CONTROL OF THE MAGNETIC PROPERTIES OF HEMIPELAGIC SEDIMENTS

Robert Karlin and Shaul Levi

College of Oceanography, Oregon State University, Corvallis

Abstract. Owing to their high sedimentation rates and wide areal extent, hemipelagic sediments along continental borderlands are potentially important high-resolution recorders of geomagnetic secular variation. To assess this possibility, we studied suboxic hemipelagic muds from the Oregon continental slope and anoxic laminated diatomaceous oozes from the Gulf of California. These sediments were rapidly deposited, with average sedimentation rates of 121 and 135 cm/kyr, respectively. Bulk sediment sedimentological and geochemical analyses indicate that the two areas represent contrasting depositional regimes. The remanence in both environments resides in fine-grained magnetite particles, although minor amounts of hematite were observed in the topmost Gulf of California sediments. Despite first-order differences, the sediments from both areas show similar downcore patterns of systematic increases in solid sulfur (mainly as pyrite), dramatic decreases in natural (NRM), anhysteretic, and isothermal remanent magnetization, intensities, and accompanying shifts in the magnetic stabilities. These changes are consistent with reduction and dissolution of the ferrimagnetic iron oxides with depth due to early diagenesis of organic matter. The magnetic grain size distribution first appears to rapidly coarsen downcore as the smallest and most abundant grains are removed, then slowly grows finer as the remaining particles dissolve. No evidence was observed for authigenic formation of magnetite. Provided sufficient concentration and stability of the detrital magnetic particles, paleomagnetic directions can survive this dissolution diagenesis. However, relative paleointensity determinations based on normalization of NRM by concentration in related parameters will give erroneous estimates of paleofield behavior in such diagenetically altered sediments.

Introduction

Geomagnetic secular variation (GSV) and paleointensity studies are important in understanding the nature of geodynamo behavior. Knowledge of the temporal and spatial distribution of the secular variation could resolve nagging uncertainties as to the validity of the axial dipole hypothesis [Wilson, 1971; McElhinny and Merrill, 1975], which is central to the tectonic reconstructions of continental blocks.

Geomagnetic spot readings are available from archaeomagnetic measurements for the past 10^4 years and from dated lava flows. However, rapidly deposited sediments afford the only continuous record of magnetic field history prior to observatory measurements during the last three centuries. Much of our present information on GSV is restricted to temperate latitudes and comes from glacially derived lakes, usually less than 20,000 years old. The lake records vary greatly in quality, due largely to their heterogeneous lithologies and discontinuous and variable sedimentation rates. Rapidly deposited marine sediments along continental margins are another potentially valuable source of GSV information. Here, depositional environments and sedimentation rates are more constant through time than in continental areas. Moreover, such sediments are more uniformly distributed geographically, and the records are limited only by the length of core that can be recovered.

Remanence acquisition in sediments is influenced by numerous physical processes including currents, slope of the depositional surface, size distributions of matrix and magnetic particles, water content, and compaction [Verosub, 1977]. The remanence and magnetic properties of slowly accumulating abyssal sediments can also be affected by the authigenic formation of magnetic Mn-Fe oxyhydroxides and/or possible maghemitization [Kent and Lowrie, 1974; Johnson et al., 1975a; Henshaw and Merrill, 1980; Prince et al., 1980]. In continental red beds, chemical remanence from the diagenetic hematite formation may account for a significant fraction of the natural remanence [e.g., Larson and Walker, 1975]. Although sedimentary geochemists have long recognized that iron phases are highly reactive in diagenetic processes [e.g., Berner, 1970], many paleomagnetic studies of Neogene sediments, particularly in exposed continental sections, have assumed that primary remanence was acquired in a chemically inert medium. However, to obtain meaningful GSV results from sedimentary sections, the geochemical and sedimentological as well as physical processes affecting the remanence must be understood.

This paper discusses detailed geochemical, sedimentological, and rock magnetic measurements made on rapidly deposited marine sediments from a small basin on the Oregon continental slope and in the Guaymas Basin of the Gulf of California. These sediments represent distinctly different sedimentation regimes, yet both types of sediments undergo drastic but similar downcore changes in their magnetic properties. Karlin and Levi [1983] showed that downcore magnetic intensity decreases and sulfide enhancements were consistent with magnetic mineral dissolution and subsequent pyrite formation. We suggested that these processes are an integral part of a progressive sequence of diagenetic reactions related to the oxidative decomposition of organic matter. In this paper, we evaluate how such changes occur and discuss the implications

Paper number 4B5069
0148-0227/85/004B-5069$05.00

for paleomagnetism. We first examine the natural remanence, rock magnetism, and magnetic mineralogy of the sediments to assess the nature of the magnetic species and their behavior downcore. We then examine the sedimentology and geochemistry of each depositional regime in order to evaluate the possibility that major changes have occurred in sediment sources. The combined analyses allow us for the first time to partition quantitatively the various iron phases in the sediments. Finally, we speculate on how similar diagenetic processes might be recognized in other sedimentary environments.

This study provides a framework for understanding postdepositional downcore changes in magnetic properties in organic-rich, hemipelagic sediments. This near-surface alteration is probably the minimum geochemical experience that similar sediments undergo before becoming lithified, uplifted, and exposed on land (e.g., the Miocene Monterey Formation in California). Although our measurements are restricted to marine sediments, parallel diagenetic alteration might also occur in organic-rich "gyttjas" commonly found in freshwater lakes.

Methods

Sediments from both areas were collected with either a 3 to 5-m Kasten corer with a 15 x 15 cm cross section or a 30 x 30 x 50-cm Reineck corer. One 450-cm Kasten core (BAM 80 E17) was studied from the Guaymas Basin, and three cores were studied from the Oregon area: Kasten cores W7710-28 (388 cm) and W7710-26 (300 cm) and Reineck box core W7809-27 (30 cm). Cores 26 and 27 are from the same location and are considered together here because the top 30 cm of core 26 was lost due to overpenetration. For the Kasten cores (E17, 28, and 26), barrel tops were sealed with polyurethane to prevent loss of surface sediment. Cores were slabbed into 5 x 15 x 50 cm trays and kept wet and refrigerated during transport and storage. At each horizon, several grams of material were freeze-dried, disaggregated in a ball mill for 5 min then split into fractions for X ray fluorescence spectroscopy (XRF), organic carbon, LECO sulfur, X ray diffraction (XRD) and Mossbauer studies. All subsamples were taken from the interiors of the cores to avoid disturbances and contamination. Paleomagnetic sampling was done with a thin-walled, square stainless steel tube mounted in an orienting frame from which material was extruded into 6.5 cm^3 boxes. Care was taken to keep samples wet, cold, and in a low field environment prior to and between measurements in order to minimize drying and viscous remanence effects.

For X ray diffraction determinations, random mounts of bulk sediments, solvated in ethylene glycol, were prepared with a 10% boehmite internal standard and analyzed on a Norelco diffractometer using Cu-Kα radiation from 3° to 60° 2θ in 0.02° steps. Room temperature Mossbauer spectra were obtained from a conventional constant acceleration spectrometer, with a ^{57}Co source diffused in rhodium, and calibrated with iron foil.

XRF measurements were made on desalted and acid-treated samples. These treatments consisted of dissolving and shaking the dry sediment in distilled water or hot 0.1N HCl for 15 min, centrifuging and pouring off the supernatant fluid. The material was washed in distilled water at least 3 times, freeze-dried, disaggregated, and compacted into planchettes with a cellulose backing for XRF analysis. Analytical uncertainty, based on calibration standards, was estimated to be <3% for Mg, Si, K, Ca, Ti, Fe, and S; <5% for Al, Mn; and <6% for P and Ba. For replicates from the same horizon and duplicated measurements, sample variability was <2% of the sample mean value. For core 28, the mean sum of oxides was 84.7% ± 0.6% and for E17, 79.8% ± 1.4%; thus the elemental analyses accounted for similar total abundances in each sample.

Initial sulfur determinations were made on a LECO sulfur analyzer. These measurements were then used to calibrate XRF sulfur counts from splits of the same samples ($r^2 = 0.99$) so that more detailed sulfur profiles could be obtained. Organic carbon and carbonate for cores E17 and 28 were measured on a LECO carbon analyzer using standard burning techniques for organic carbon and a hot phosphoric acid treatment for carbonate [Weliky, 1982].

Remanence measurements were made on a Schoenstedt DSM-1 spinner magnetometer for the Oregon (OR) sediments and on a SCT cryogenic magnetometer for the Gulf of California (GC) samples. All stepwise alternating field (af) demagnetizations were done with a single axis Schoenstedt af demagnetizer up to at least the sample's median demagnetizing field (MDF), which is the peak af value where one half of the original remanence remains. Anhysteretic remanent magnetizations (ARM) were produced with 1000 Oe (1 Oe = 0.1 mT) af superimposed on parallel DC biasing fields of 0.50 Oe for the OR sediments and 0.25 Oe for the GC sediments. No ARM anisotropy was observed, and ARM acquisitions were linearly proportional to the applied bias field up to 2 Oe with no change in MDF. Fourteen samples from OR core 28 and 12 samples from GC core E17 were also given stepwise isothermal remanent magnetizations (IRM) to 10 kOe, followed by af demagnetization to 1000 Oe af in 50 to 100-Oe steps.

The magnetic components of seven samples from OR cores 28 and 27 and GC core E17 were separated using a 3-kOe electromagnet and a closed, continuous flow-through system [Karlin, 1984]. Although extractions took 4-7 days, ~40% of the IRM and ~70% of the ARM remained in the residue after separation. The remanences of the residues showed higher MDF's than in the untreated sediments, suggesting that physical separation preferentially extracts the coarser magnetic components. The magnetic separate mineralogy was established using a conventional Debye-Scherrer X ray powder diffraction camera with Co radiation (35 kV, 18 mA), an Fe filter, and 0.3-mm capillary tubes. A minimum of three peaks was considered necessary for positive mineral identification. The textures and qualitative compositions of the magnetic separates

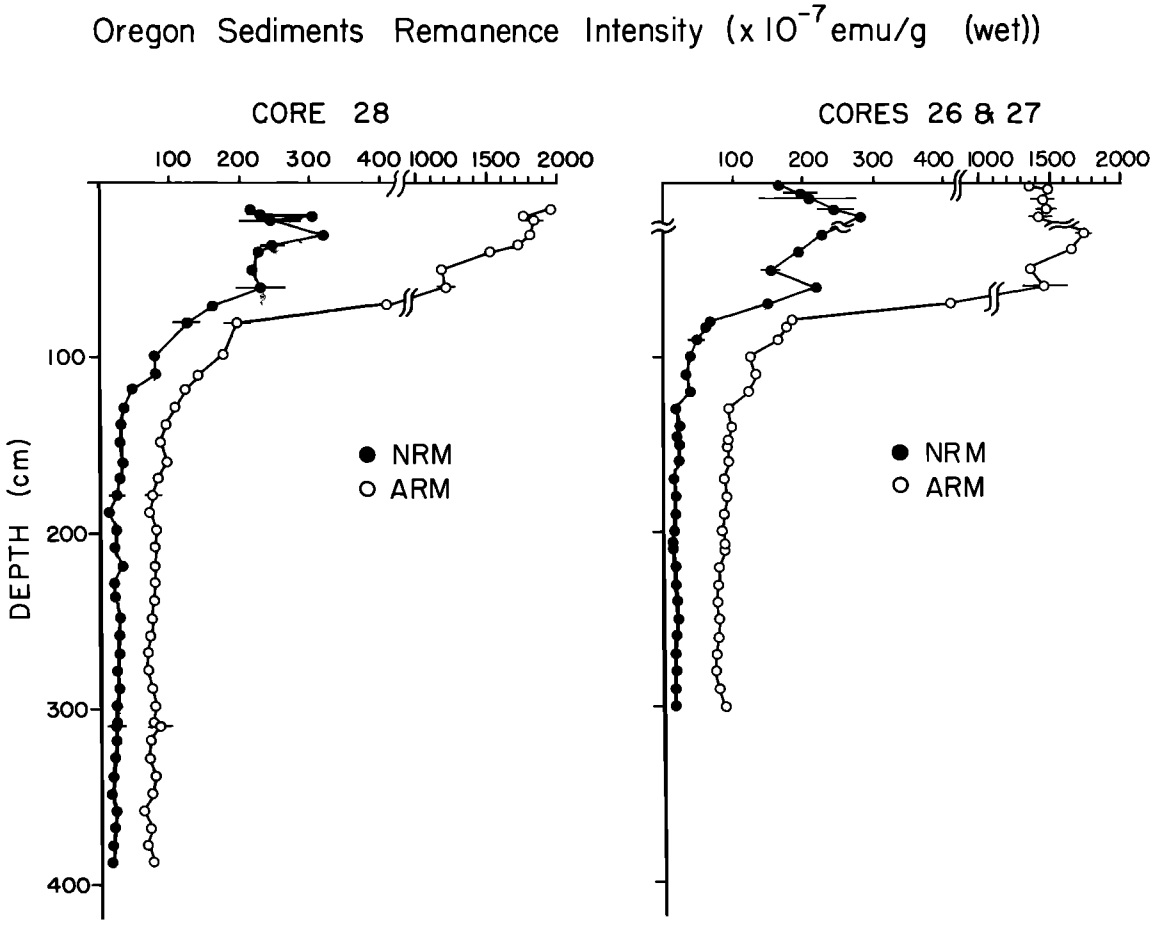

Fig. 1. NRM and ARM profiles of OR core 28 and OR cores 27+26 sediments. NRM (solid) and ARM (open) values have been af demagnetized to 150 Oe. The break in the depth axis at 30 cm of Figure 1b denotes the boundary between cores 27 and 26.

were examined using a scanning electron microscope (SEM) with an attached energy dispersive X ray unit (EDAX).

Results

Oregon (OR) Sediments

Sediments from our study area in a small basin on the Oregon lower continental slope (44°50'N, 125°8'W, 1820 m water depth) are typical olive green, heavily bioturbated, suboxic hemipelagic muds composed of 30-40% clay, 40-60% silt, and minor amounts of sand. Eleven ^{14}C ages for the 300-cm Kasten core 26 and 30-cm Reineck core 27 increase linearly with depth (r^2 = 0.95), yielding a mean sedimentation rate of 121 ± 10 cm/kyr with a surface intercept at 2017 ± 290 years. Four ^{14}C ages from the 388-cm Kasten core 28 follow an identical trend.

Regionally, muds along the Oregon continental margin are highly terrigenous mixtures derived mainly from Oregon and northern California sources [Duncan, 1968; Kulm and Scheidegger, 1979; Karlin, 1980]. The surface sediments in our study area contain significant portions of smectite from volcanogenic soils in the Columbia River Basin, chlorite from the metamorphic rocks in the Klamaths and California Coast Ranges, hornblende from the Klamaths, as well as ubiquitous quartz, biogenic opal, and illite [Karlin, 1980; Krissek, 1982]. The chemical characteristics of the source assemblages are not well defined [Krissek, 1982], and, to date, no downcore geochemical profiles have been reported.

Rock Magnetism. Downcore profiles of natural remanent mangnetization (NRM) and ARM intensities, demagnetized at 150 Oe af, for Oregon cores 28 and 27+26 (Figure 1) show very similar characteristics. (Cores 26 and 27 are considered together because Kasten core 26 overpenetrated by 30 cm and Reineck box core 27 came from the same location.) In the top 60 cm of cores 28 and 26, as in all of core 27, NRM intensities are high and somewhat variable. Between 60 and ~120 cm, NRM intensities decrease monotonically by almost an order of magnitude. Below 120 cm, intensities continue to decrease but at a much slower rate, and variability is much less. This precipitous decrease in NRM is obviously not produced by changes in the earth's field since the concentration dependent ARM and IRM profiles show similar but even more pronounced behavior.

The stability of the remanence can be roughly characterized by the median demagnetizing field (MDF), In general, higher MDF's indicate a lesser contribution of relatively larger multi-

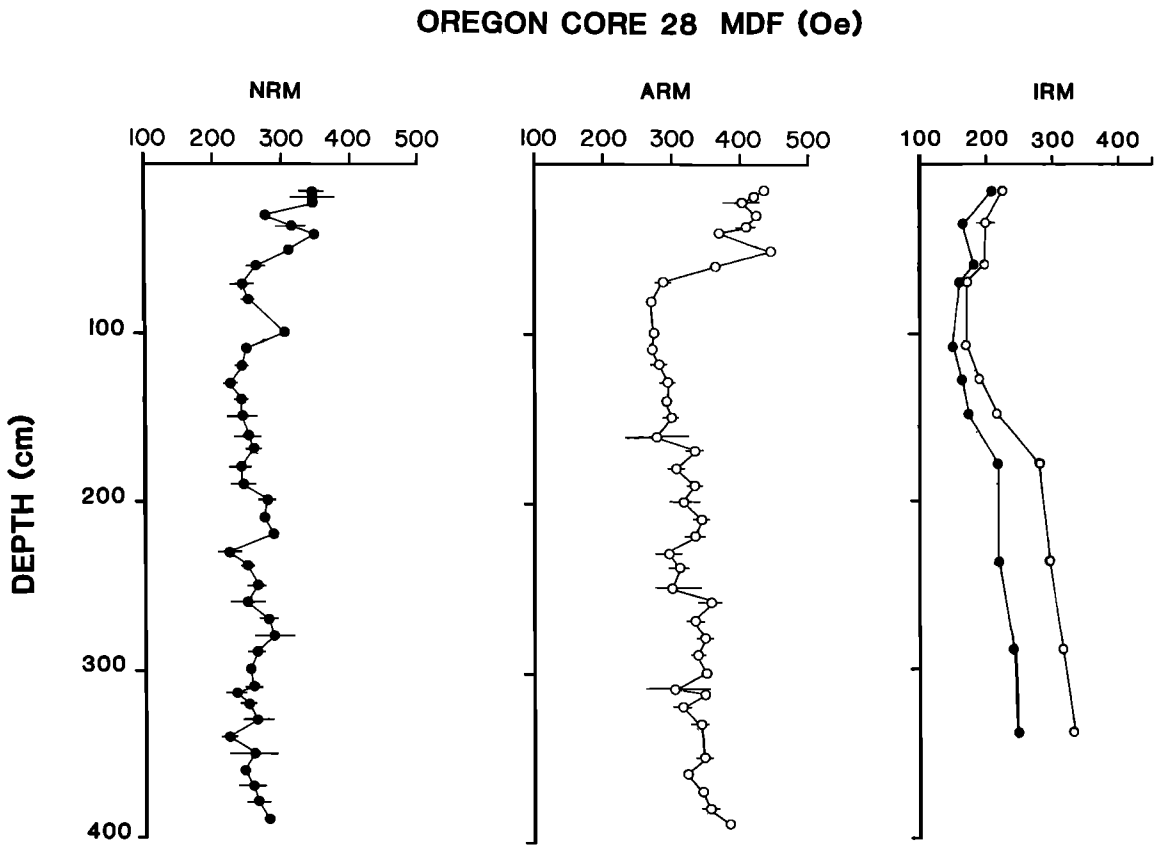

Fig. 2. Downcore profiles of NRM, ARM, and IRM median demagnetizing fields (MDF's) for core 28. ARM's were produced at 1 kOe af with a biasing field of 0.50 Oe and IRM's at 5 kOe. In Figure 2c, solid circles denote MDF's with their 1 kOe af values removed; open circles are uncorrected.

domain (MD) particles. As in the intensity profiles, all of the Oregon sediments show similar downcore trends in MDF values of NRM, ARM, and IRM (Figure 2). In core 28, NRM MDF's decrease from 300-400 Oe in the top 60 cm to values of 230-280 Oe below this depth. ARM MDF's are higher than corresponding NRM or IRM MDF values. The core 28 ARM MDF profile shows values of 350-450 Oe in the top 60 cm, lower values of 280-300 Oe from 60 to 160 cm, and slightly higher values of 300-370 Oe deeper in the core. The ARM MDF's of cores 27+26 show an identical pattern. Overall, the relatively high NRM and ARM stabilities in the Oregon sediments imply that the remanence is controlled by single-domain (SD) and pseudo-single-domain (PSD) particles [Levi and Merrill, 1976], as magnetite was found to be the dominant magnetic carrier (see next section).

The af demagnetization curves of NRM, ARM, and IRM are shown for the representative levels of core 28 in Figure 3. The samples show consistent trends with depth. For the highly magnetized samples in the top 60 cm, ARM, and, to a lesser extent, NRM are much "harder" than IRM. The high NRM stabilities and lower stabilities of IRM relative to NRM or ARM suggest that the depositional remanent magnetization (DRM) initially resides mainly in fine SD and PSD grains [Johnson et al., 1975b]. In the intermediate intensity region between 70 and 150 cm, the MDF's of all three remanences decrease, implying that the remanence is produced by a coarser fraction than in the top 60 cm. ARM and NRM curves are still more stable than IRM. For the low-intensity samples below 150 cm, ARM and IRM curves are similar, and their MDF's show an apparent increase with depth, whereas the NRM MDF's remain essentially unchanged. On the basis of these trends the ARM and IRM seem to be controlled by progressively finer particles at depth.

Although the relevance of the paleomagnetic directions with regard to secular variation will be discussed in a later paper, the reliability of the directions is germane to our examination of the rock magnetism. All of the Oregon sediments showed exceptional directional stability and smooth decay upon af demagnetization (AFD) to at least 400 Oe peak field. Overall, the angular mean standard deviation between the 100, 150, and 200 Oe af levels averages 1.5° and 1.4° per sample for cores 28 and 26, respectively. At each horizon, mean directions were obtained by vector averaging the 100, 150, and 200 Oe af levels of each sample then combining samples into a horizon average. For core 28 the core mean inclination (Ic) is 62.6° with an α_{95} of 2.7° and k of 65.5. For core 26, Ic is 60.6° with an α_{95} of 1.8° and k of 202. (The k is the

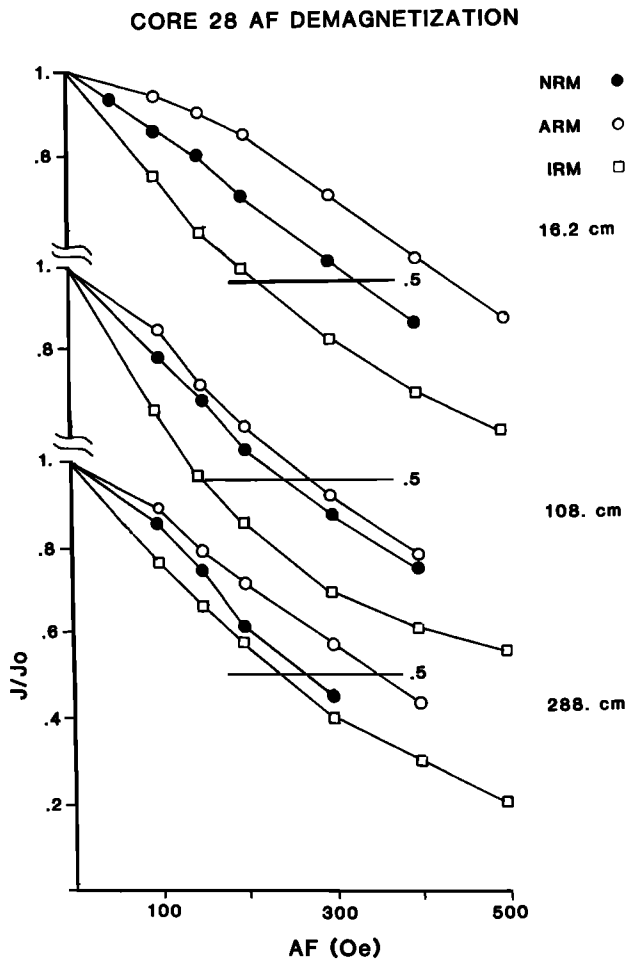

Fig. 3. Normalized demagnetization curves of NRM, ARM and IRM for core 28 sediments. ARM were given at 1 kOe af with a biasing field of 0.50 Oe, and IRM's were produced at 5 Oe. IRM's have their 1 kOe af value subtracted.

best estimate of the precision parameter, and α_{95} is the angular radius of the 95% cone of confidence of the Fisher distribution [Fisher, 1953]). The expected geocentric axial dipole (EGAD) inclination at this latitude is 63°, thus the EGAD inclination and the mean inclinations of both cores match fairly closely.

The within and between horizon variability can be partitioned using a two-tier analysis of variance (ANOVA) approach [Watson and Irving, 1957]. This technique assumes that within horizon variability is Fisherian and independent of depth. Because of suspected sampling disturbance, the 147-cm level of core 26 was excluded from the analysis. Tables 1 and 2 summarize the ANOVA results for both cores. Ratios of between and within horizon mean squares yield F ratios of 6.2 for core 28 and 4.1 for core 26. These values far exceed the table F value at a 0.01 significance level for the appropriate degrees of freedom. This suggests that the between horizon SV significantly exceeds the within horizon variability due to the sedimentary recording process and random errors in sampling. Moreover, the average within horizon angular standard deviations above and

TABLE 1a. Core 26 Summary Statistics (30-300 cm)

	N	$\bar{I}$(°)	$\bar{D}$(°)	α_{95}(°)	k	s(°)
By horizon	30	60.6	165.3	1.8	205	5.7
All Samples	93	60.4	165.5	1.2	160	6.4

The af levels of 100, 150, 200 Oe have been vector averaged for each sample. N, population size; $\bar{I}$, inclination and $\bar{D}$, declination of mean paleomagnetic direction; α_{95}, k are statistical parameters, [Fisher, 1953]; s, angular standard deviation of the vector mean.

below the reduction zone are comparable (3° ± 1.4° versus 4.0° ± 1.7° in core 26). Thus, although the rock magnetic properties of these cores show substantial downcore variation, the directions are stable and replicable and appear to record faithfully the ambient field.

Magnetic Mineralogy. From XRD of the magnetic separates, the only ferrimagnetic species identified in the OR sediments was pure magnetite with a unit cell parameter of a_o = 8.39 ± 0.01 Å. Other nonmagnetic minerals included chlorite, quartz, plagioclase, and possibly hornblende. Reflections from magnetic sulfides such as pyrrhotite and greigite were not observed.

SEM photomicrographs of core 28 magnetic separates from 40-50 cm and 333-343 cm (Figure 4) showed, in order of abundance, clay platelets (<2-20 μm) > large (>20 μm) silicious biogenic fragments (mostly diatoms) > plagioclase, quartz > magnetite dipyramids and unidentified anhedral grains. Clumps of clay particles with very small (<2 μm) subhedral to euhedral magnetite crystals were common, especially in the 40-50 cm sample. EDAX scans of the surfaces of diatom and quartz fragments showed Fe and Si peaks, while clay platelets gave high Fe as well as Al and Si peaks. This suggests that the surfaces of the nonmagnetic particles were covered with an Fe-rich film whose colloidal particles were too fine to resolve. EDAX scans of magnetite euhedra showed only Fe, consistent with the cell parameters of a pure Fe_3O_4 magnetite, as determined by XRD.

An obvious feature of the core 28 SEM photos was that the grain sizes of the 40-50 cm sample were finer than for the 333-343 cm sample. Whereas the top sample contained many fine grains <1-2 μm in diameter as clusters and affixed to larger fragments, the deeper sample had

TABLE 1b. Core 26 Variance Analysis (30-300 cm)

	degs. of freedom	Mean Square	F	k	s(°)
Within horizon	126	1.58×10^{-3}	4.1	316	4.6
Between horizons	58	6.48×10^{-3}		338	4.4

See Table 1a for for explanations.

TABLE 2a. Core 28 Summary Statistics (16-388 cm)

	N	$\bar{I}$(°)	$\bar{D}$(°)	α_{95}(°)	k	s(°)
By horizon	42	62.6	253.1	2.7	66	5.0
All Samples	90	61.1	251.1	1.8	72	8.7

The af levels of 100, 150, 200 Oe have been vector averaged for each sample. See Table 1a for explanations.

a more uniform distribution with numerous individual 5-20 μm magnetite euhedra and only a few obvious micron-sized particles. IRM acquisition experiments on several samples from core 28 (Figure 5) showed saturation by 3-5 kOe, suggesting that the magnetic properties of the Oregon sediments were controlled by magnetite [Dunlop, 1972].

X ray diffraction and Mossbauer spectroscopy. X ray diffraction and Mossbauer spectroscopy were undertaken to ascertain the nature and downcore variability of the terrigenous fraction in order to assess whether any major changes in sediment source had occurred. Stacked X ray diffractograms of bulk sediments from five levels of core 28 are presented in Figure 6. For all levels, major peaks, in order of decreasing dominance, included quartz, chlorite, illite, montmorillonite (smectite), plagioclase, amphibole, and olivine. Minor peaks of pyrite were detected in the samples from 130 and 237 cm. Overall, the mineralogy and relative peak heights showed very little variability downcore, suggesting that the relative inputs of the different terrigenous sources did not change significantly over time.

Mossbauer spectroscopy (for review, see Bancroft, [1973]) was used to examine the oxidation state and chemical structure of the iron-bearing minerals. Well resolved Mossbauer spectra were obtained for samples from 14 levels of core 28. Samples from all depths gave essentially identical spectra (Figure 7), with a large absorption peak at -0.2 mm/s, a distinct shoulder at 0.6 mm/s, and a prominent secondary peak at 2.44 mm/s. Magnetic hyperfine splitting was not observed, suggesting that the ferrimagnetic fraction constituted <5% of the total iron. As described by Karlin [1984], the spectra could be optimally fit with two Lorenzian couplets, giving peak pairs with comparable heights and widths. The Mossbauer parameters of one of the couplets was unambiguously identified as high spin Fe (II) in chlorite with an isomer shift (IS) = 1.12 ± 0.005 mm/s, quadrupole splitting (QS) = 2.65 ± 0.01 mm/s, and a half width (Γ) = 0.44 ± 0.01 mm/s. The other couplet, with IS = 0.36 ± 0.01 mm/s, QS = 0.62 ± 0.02 mm/s, and Γ = 0.65 ± 0.04 mm/s, was probably a mixture of high spin Fe (III) in mainly illite, with lesser amounts of ferric gel, poorly crystalline geothite, and/or pyrite.

We attempted to resolve the second couplet by creating a calibration curve using mixtures of pyrite and Fe (III)-rich chlorite standards. However, we were unable to resolve the spectral overlap between the pyrite Fe (II) and chlorite Fe (III) doublets without constraining peak positions, which we think is unreasonable. Thus, where both species coexist [e.g., Suttill et al., 1982], quantitative estimation of pyrite or ferric oxide percentages using Mossbauer spectroscopy is questionable.

Mossbauer spectra of clay separates were essentially identical to the bulk sediment except that the total absorption area in the clay separates was much larger. By comparing the relative absorption areas of the various spectra, ~75% of the iron in the sediments was found to reside in the clay-sized fraction.

The proportion of the chlorite couplet to the total absorption area (0.557 ± 0.014) in the bulk sediments was remarkably constant for all levels of core 28. The downcore invariance of the iron in the chlorite fraction is consistent with the XRD results, suggesting that the provenance of the terrigenous mineralogy has not changed significantly through time.

Elemental abundances. The sediments from core 28 show monotonous profiles in their major element chemistry (Figure 8). The mean values and variabilities for 11 major elements (normalized as oxides to 100%) are summarized in Table 3. With the exception of S, CaO, org C, and BaO the remainder of the elements show downcore variabilities of less than 5%. (The index of variability, percent variation, V, is defined here as 100 x standard deviation/mean for each element [Snedecor and Cochran, 1980]). Interelement correlations (top half of Table 4) show strong positive associations of sulfur with depth (r = 0.84) and weaker correlations of Al with Ti (0.65), Mn (0.68), Fe (0.61), and P (0.62). Negative correlations are found between Si and Ti (-0.67), Mg (-0.73), and Mn (-0.70) as well as P with depth (-0.69) and S (-0.75). The associations between depth, sulfur, and P can be attributed to oxidative decomposition of organic matter and the formation of sulfides with depth [Karlin and Levi, 1983]. The correlations between the terrigenous elements Al, Ti, and Mn are probably due to their association with clay minerals. Since Si is found in biogenic opal as well as terrigenous silicates, the weak negative Si correlations could reflect fluctuations in biogenic versus terrigenous input but also may be partly an artifact of a closed data set.

Upon acid treatment of the core 28 samples with 0.1N HCl, downcore trends, mean values, and variabilities remained unchanged for Si, S, and the terrigenous elements Al, K, Ti, Mn, and Fe. However, 46% of Ca, 42% of total P, 22% of Ba, and 8% of Mg were removed. Two fluctuations in

TABLE 2b. Core 28 Variance Analysis (16-388 cm)

	degs. of freedom	Mean Square	F	k	s(°)
Within horizon	108	2.30×10^{-3}	6.2	217	5.5
Between horizons	70	1.42×10^{-3}		110	7.7

Six horizons with single samples are excluded. See Table 1a for explanations.

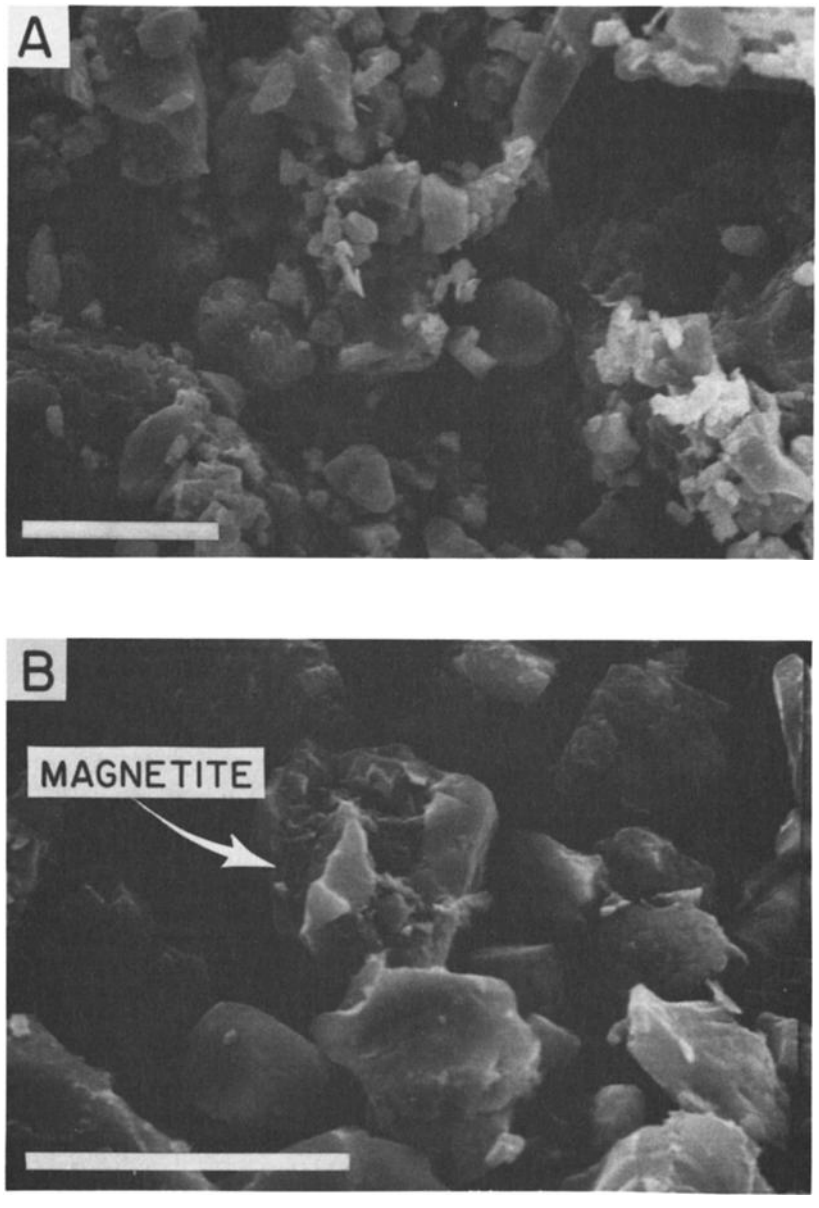

Fig. 4. (a) SEM photomicrographs of magnetic separates from core 28, 40-50 cm. Note the large number of ≤2 μm particles affixed to larger grains. (b) For depths 333-343 cm, the overall grain size is generally coarser than in the separates from 40-50 cm. Large 10 to 50-μm magnetite octahedra are deeply eroded. The bar in each photo is 10 μm long.

Ca at 100 and 130 cm were lost upon acid treatment; thus these variations were probably caused by minor fluctuations in biogenic carbonate input.

If the organic carbon were readily metabolizable and only sulfate reduction occurred, we would expect that oxidative decomposition of organic matter should result in organic carbon curves which mirror the sulfur profiles. Although organic carbon generally decreases downcore (Figure 8) and sulfur increases (Figure 8) the shapes of the curves do not match closely, implying that the reservoir of metabolizable carbon utilized in sulfate reduction is not simply related to the total residual carbon in the system.

Of all of the elements, sulfur shows the strongest concentration gradient with depth. Karlin and Levi [1983] showed that the downcore sulfur increase can be related to the formation of sulfides due to the progressive oxidative decomposition of organic matter and the reduction of iron and seawater sulfate with depth. When compared to sulfur in pore water sulfate (0.1-0.2% dry weight for 60% water content) and similar surface solid sulfur values, the downcore solid sulfur for cores 28 (0.6%) and 26 (0.5%) shows an excess, suggesting cycling of seawater sulfate through the sediments. This excess downcore solid sulfur has often been observed in other anaerobic marine sediments [Goldhaber and Kaplan, 1974; Berner, 1981b].

In marine sediments, commonly occurring sulfur minerals include pyrite (FeS_2), mackinawite

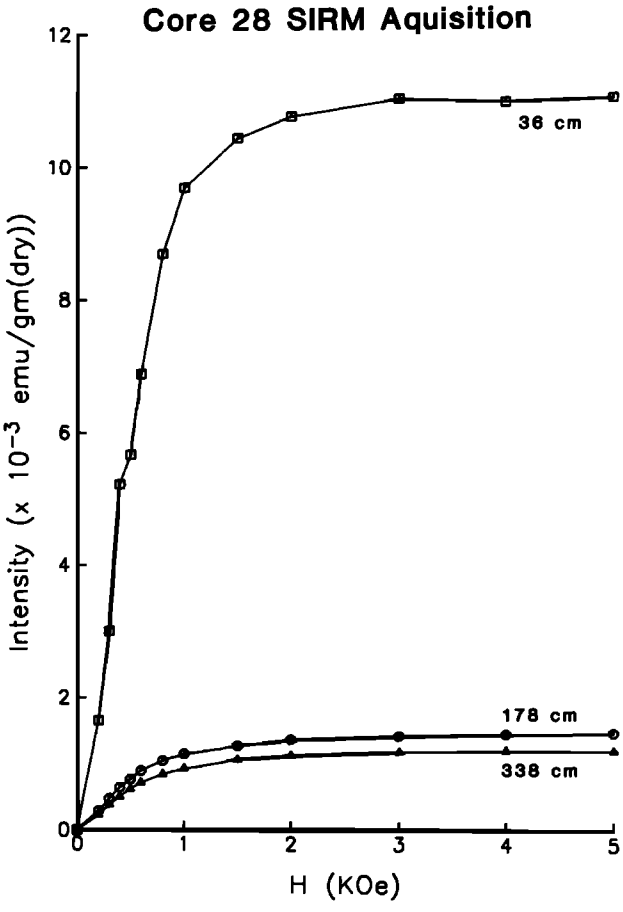

Fig. 5. Acquisition curves for saturation isothermal remanence (SIRM) at different depths for OR Core 28 sediments.

(FeS) barite ($BaSO_4$), and Mn sulfide [Goldhaber and Kaplan, 1974; Berner, 1981b; Suess, 1979a, b]. In core 28 the lack of change of S and Fe upon acid treatment suggests that acid soluble monosulfides, such as the metastable species mackinawite, were not present in measurable quantities. If all of the Mn were in a sulfide form, the Mn sulfide could account for <5% of the downcore solid sulfur. Sulfur associated with barite could account for ~6% of the total sulfur in the top meter but only about 3% in the deeper parts of the core if all of the Ba is in barite form. Assuming that organically bound sulfur is negligible, about 90-95% of the solid sulfur must occur as pyrite.

Chemical analyses of cores 27 and 26 were undertaken to examine whether intercore correlations could be made independent of the paleomagnetism of the sediments. Overall, downcore variabilities were similar between cores 27+26 and core 28. However, downcore trends in cores 26 and 27, with the exception of S, showed no obvious correlation to core 28. While variability in Ca in both data sets was of the order of 10% and fluctuations occur at similar levels, a definitive correlation based on Ca is equivocal. When normalized to Al_2O_3, with the exception of S and CaO, the remainder of the elements were essentially constant downcore. Thus downcore changes would seem to be largely a result of fluctuating biogenic input and perhaps minor downcore differences in grain size.

The lack of definitive downcore chemical correlation between cores 28 and 27+26 (which are within 1 km of each other) is problematic. Since the variability for most elements in both cores is less than 5%, an obvious conclusion from the chemistry is that with the exception of diagenetic S and biogenic carbonate, the sediments are very homogeneous. The monotony of the sediment chemistry is a mixed blessing. While making these cores excellent for paleomagnetism, the homogeneity also inhibits stratigraphic correlation.

Partitioning of Iron. By combining chemistry, X ray diffraction, and Mossbauer and rock magnetic studies, we can partition the iron found in the core 28 sediments into different phases. We assume that no appreciable ferric iron is present in the chlorite and that pyrite iron can be estimated from the solid sulfur, which is composed solely of pyrite and barite. Since the predominant magnetic mineral is magnetite, we can estimate the amount of iron locked in magnetites from the saturation remanence (SIRM) of each sample and the spontaneous magnetization of magnetite (92 emu/g). For this calculation we assume that the SIRM/saturation magnetization ratio is equal to 0.1, a value typical of magnetites with similar stabilities [Levi and Merrill, 1978].

Through XRD, Fe-rich trioctahedral chlorite was identified by its basal 00ℓ reflections [Brindley and Brown, 1980] as the dominant iron bearing detrital mineral. The Mossbauer spectra suggested that Fe (II) in the chlorite constituted 56 ± 1% of the total iron. Thus the average iron content in chlorite is 2.42 ± 0.06%, while 1.93% is present in illites, smectites, ferric oxides, and pyrite. Since the average acid insoluble sulfur content is 0.42 ± 0.16%, average pyrite iron content must be ~0.49%. Thus 20-25% of the second Mossbauer couplet is due to Fe (II) in pyrite. If we assume that the remainder of the iron is due to Fe (III) in clays and oxides, the ferrous/ferric ratio for the core is (2.91/1.44) = 2.02. This indicates that about 2/3 of the iron minerals in this core are

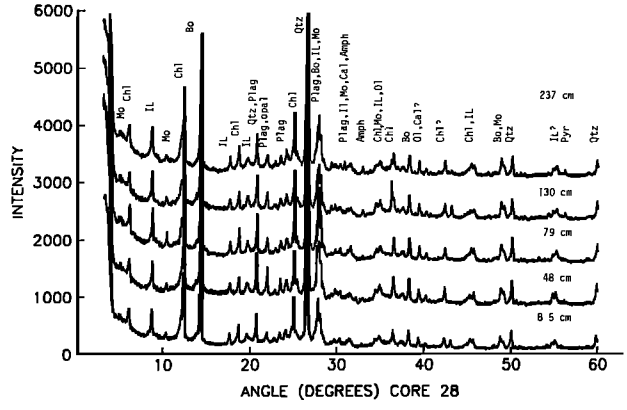

Fig. 6. Stacked X ray diffractograms of five levels from core 28. The x axis is the diffraction angle (2θ) in degrees. Glycolated random mounts included a 10% boehmite standard. Diffraction peak identification is Mo, montorillonite (smectite); Chl, chlorite; IL, illite; Bo, boehmite; Qtz, quartz; Plag, plagioclase and feldspars; Cal, calcite; Amph, amphibole; Ol, olivine; and Pyr, pyrite.

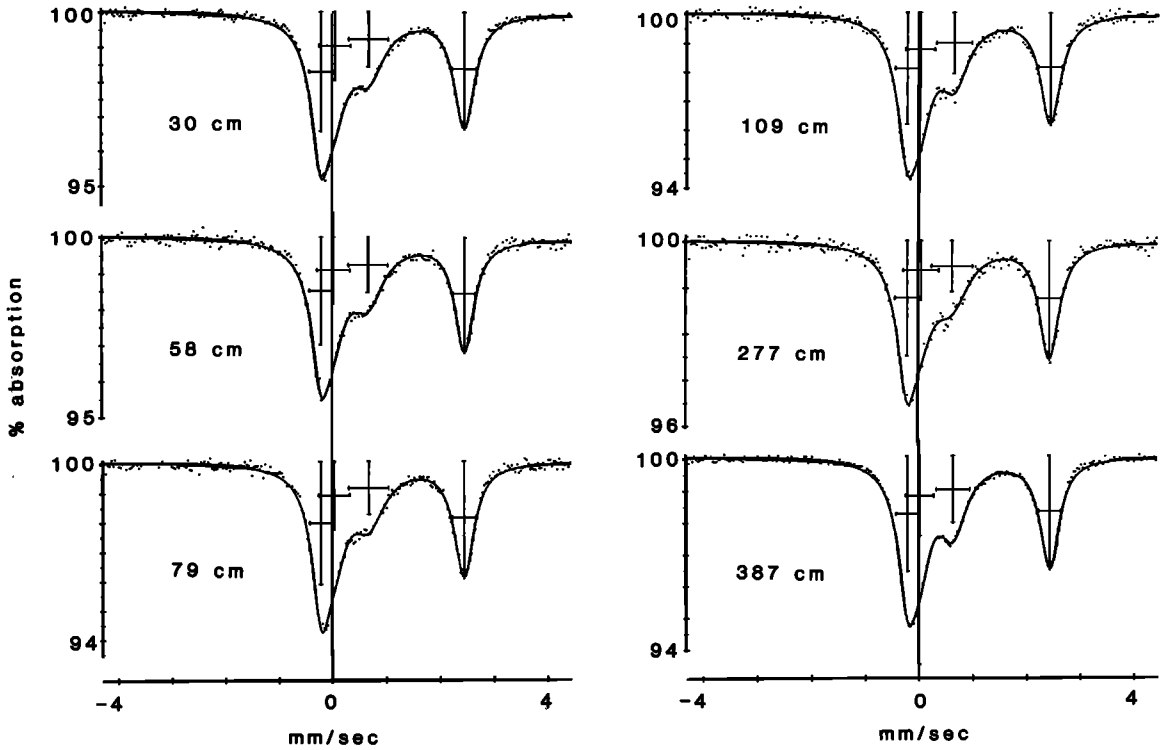

Fig. 7. Mossbauer spectra at room temperature of bulk sediments from six levels of Oregon core 28. Vertical axis is percent absorption. The smooth curve is the fitted spectrum using two unconstrained Lorenzian peak pairs. The heights and line widths of each peak are shown by vertical an horizontal bars. Note the essential similarity of the spectra.

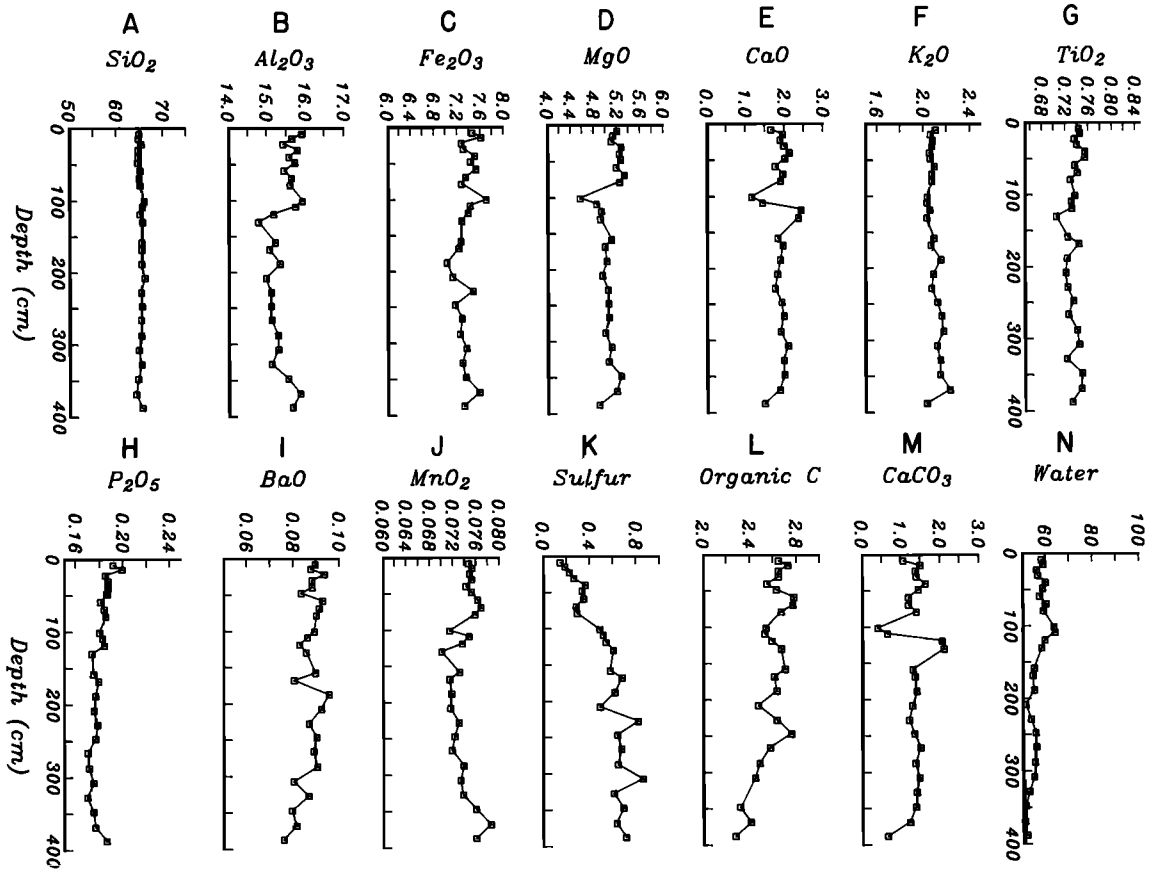

Fig. 8. Oregon core 28, downcore profiles of major element chemistry, organic carbon, $CaCO_3$, and water contents. Abundances are given as oxides in percent dry weight and are normalized so that the sum of the oxides of the 12 major elements equal 100%.

TABLE 3. Oregon Core 28: Summary of Chemical Analyses

	Oxide Abundances			Ratios to Al_2O_3		
Oxide	Mean	SD	%V	Mean	SD	%V
SiO_2	65.123	0.455	0.7	4.223	0.105	2.5
TiO_2	0.735	0.012	1.6	0.048	0.001	1.6
Al_2O_3	15.429	0.320	2.1	1.0	-	-
Fe_2O_3	7.347	0.159	2.2	0.476	0.009	1.8
MnO	0.074	0.002	2.7	0.005	0.0001	2.1
MgO	5.078	0.171	3.4	0.330	0.011	3.4
CaO	1.864	0.240	12.9	0.121	0.017	13.8
K_2O	2.091	0.049	2.3	0.136	0.004	3.2
P	0.180	0.007	3.9	0.012	0.0004	3.1
BaO	0.087	0.005	5.7	0.006	0.0004	6.2
S	0.505	0.199	39.4	0.033	0.013	39.4

Abundances are normalized to sum = 100% of oxides. Samples were desalted prior to treatment. SD = standard deviation. The percent variation, %V, is a measure of variability and is defined as 100 x SD/mean.

in a reduced state, with the major phase being in detrital chlorite.

The resulting profile of iron phases downcore (Figure 9) shows the essential constancy of total Fe and chlorite with depth. Although the top few centimeters of core 28 (and 26) are missing, the lack of a downcore concentration gradient in Fe implies in situ reduction of iron oxides and transformation to acid insoluble pyrite rather than upward diffusion of porewater Fe (II) and reprecipitation near the oxic/anoxic boundary. While chlorite makes up about 56% of

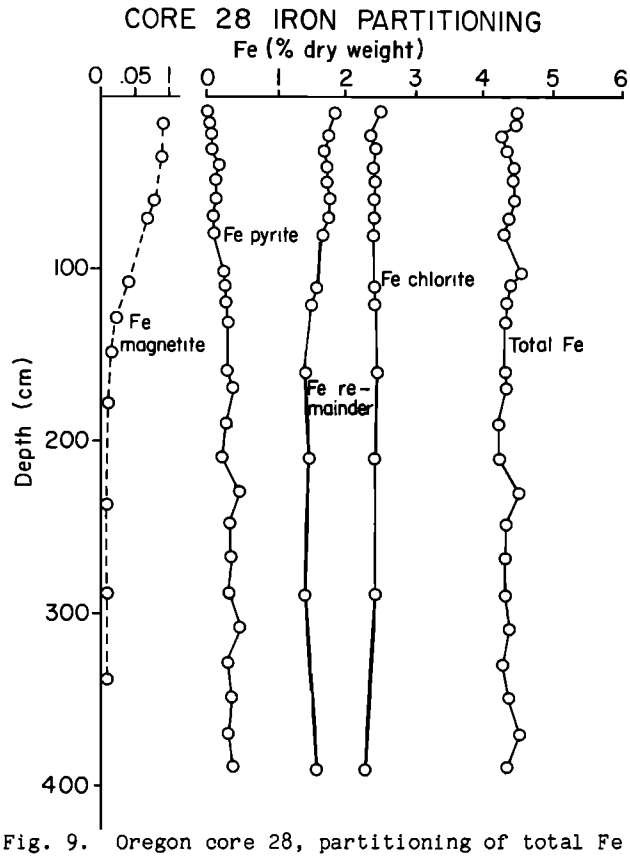

Fig. 9. Oregon core 28, partitioning of total Fe into magnetite, chlorite, pyrite, and residual phases.

the total Fe, pyrite iron accounts for about 3-5% in the top meter and 10-14% deeper in the core. The remaining Fe (25-40%) must be in the form of resistant oxides (e.g., spinels, magnetite), other detrital silicates (e.g., pyro-

TABLE 4. Oregon Core 28: Correlation Matrix of Oxide Abundances

	Depth	Na	Mg	Al	Si	P	K	Ca	Ti	Mn	Fe	Ba	S	Sum	H_2O
Depth	+	0.61	-	-	-	-0.69	0.50	-	-	-	-	-0.52	0.84	-	-0.76
Na	0.63	+	-	-	-	-	0.55	-	-	-	-0.52	-	-	-	-0.84
Mg	-	0.49	+	-	-0.73	-	-	0.45	0.47	0.60	-	-	-0.41	-	-
Al	-	-	-	+	-0.45	0.62	-	-0.50	0.65	0.68	0.61	-	-0.54	-	-
Si	-	0.40	-	-	+	-	-0.41	-	-0.67	-0.70	-	-	-	-	-
P	-0.67	-	-	-	-	+	-0.49	-	0.49	0.44	0.47	-	-0.75	-	0.48
K	0.57	0.70	0.48	-	0.58	-0.51	+	-	-	-	-	-	-	-	-0.55
Ca	-	-	0.71	-	0.43	-	0.49	+	-	-	-	-	-	-	-
Ti	-	0.44	0.54	-	0.51	-	0.55	0.64	+	0.57	0.47	-	-	-	-
Mn	-	0.46	0.61	-	-	-	-	-	-	+	0.40	-	-0.40	-	-
Fe	-	-	-	-	-	-	-	-	-	-	+	-	-	-	0.44
Ba	-	-	-	-	0.47	-	-	-	-	-	-	+	-0.49	-	-
S	0.83	0.48	-	-	0.52	-0.58	0.54	-	-	-	-	-	+	-	-0.53
Sum	-	-	-	-	-	-	-	-	-	-	-	-	-	+	-
H_2O	-0.76	-0.84	-	-	-	0.48	-0.55	-	-	-	0.44	-	-0.53	-	+

Oxides are salt adjusted and normalized to sum = 100%. Correlations shown are significant at a 0.05 significance level ($r > 0.40$). Upper triangular matrix is interelemental correlations of oxides. Lower triangular matrix contains correlations oxides/Al_2O_3. N = 26.

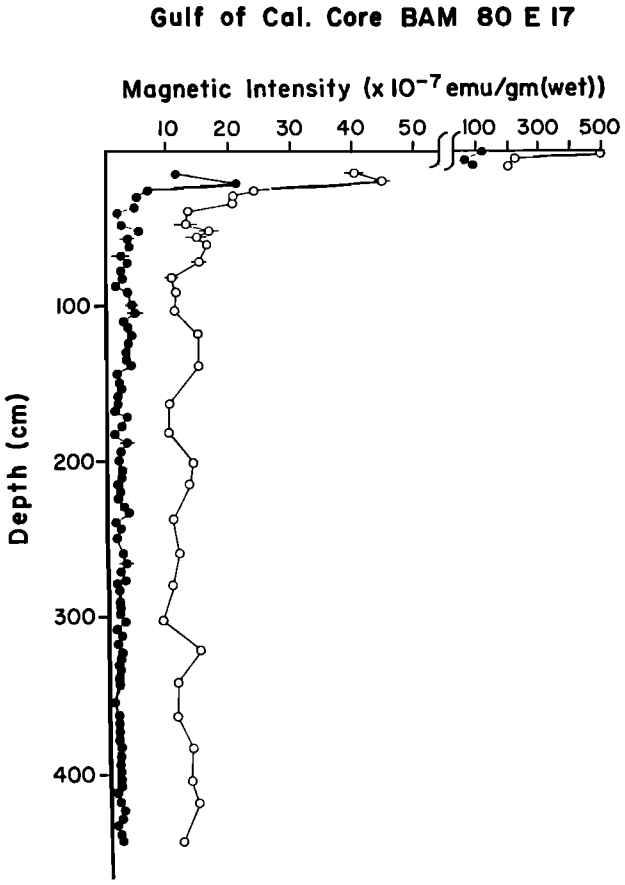

Fig. 10. NRM and ARM profiles of core E17 sediments. NRM (solid) and ARM (open) values have been af demagnetized to 100 Oe af.

xenes, amphiboles, olivines), and clay minerals (e.g., illites, smectites).

The iron in magnetite in the top 70 cm accounts for ~2% of the total iron. Below 120 cm depth, the magnetite iron content drops by an order of magnitude compared to the surface sediments. Interestingly, the magnetite iron in the surface sediments is ~20% of the pyrite iron downcore. Thus magnetite appears to be preferentially dissolved relative to the other iron phases.

Gulf of California (GC) Sediments

The sediments in our study area in the Gulf of California (27°58.5'N, 111°37.5'W, 622 m water depth) are finely laminated diatomaceous oozes, underlying a zone where the oceanic oxygen minimum intersects the slope [Schrader et al., 1980]. Strong seasonal upwelling alternating with periods of heavy rainfall and high terrigenous input produces fine submillimeter couplets of light-colored diatom rich and darker organic-terrigenous-diatom layers [Schrader et al., 1980; Calvert, 1964]. DeMaster [1979] showed that the chronologies based on laminae counts and ^{210}Pb decay curves match closely, implying that the couplets represent annual varves, at least for the past 200 years. A detailed varve chronology [Karlin, 1984] gave a base age for core E17 of ~3340 years, yielding an overall sedimentation rate of 135 cm/kyr for the entire 450-cm core. This estimate is a lower limit, since most sources of error (i.e., hiatuses, indistinct laminations) tend to underestimate the true age.

In a classic work on the distribution of sands in the gulf, Van Andel [1964] found that distinctive assemblages of heavy minerals were found proximal to their source areas (in this case the Rio Yaqui). From the sharp boundaries of the heavy mineral provinces, Van Andel concluded that in most of the central gulf, redistribution of sediments by longshore transport was minimal and most fluvial material was carried directly offshore to deep basins. At present, downcore geochemical or sedimentological analyses have not been reported for the laminated sediments of the gulf, although sulfur diagenesis in the pore waters and solid phases has been well documented [Berner, 1964; Goldhaber and Kaplan, 1980].

Rock magnetism. For the laminated sediments from GC core E17, intensity profiles of NRM, ARM (Figure 10), and IRM show a very steep decrease in magnetization from the surface to about 30 cm. Below this depth, NRM intensities continue to decrease slowly, while ARM's and IRM's are relatively constant or slightly variable with depth. NRM MDF's (Figure 11) also decrease sharply from the surface to ~20 cm and then remain relatively constant downcore. Both ARM and IRM MDF's (Figure 11) also show an initial decrease from the surface, but then slowly increase downcore.

NRM, ARM, and IRM AFD curves for the E17 core show similar but even more pronounced behavior than the Oregon sediments (Figure 12). In the top 30 cm, while intensities for all three remanences decrease dramatically, NRM stabilities drop from about 350 to 150 Oe and then stay relatively constant with depth. The high ARM and IRM stabilities in the top 20 cm indicate a dominant fine-grained component in the surface sediments. ARM and IRM stabilities initially decrease from the surface to 20 cm and then increase slowly downcore. These trends suggest an initial coarsening of the distribution followed by a gradual fining with depth.

The NRM is initially more stable than IRM in the top 30 cm, but with depth, NRM stabilities are significantly lower than either of the laboratory-produced remanences. The relatively high NRM stabilities in the top of the core imply that the DRM is initially held mostly in SD and PSD grains, but with depth, only a small fraction of the original detrital remanence survives and this is carried by relatively more MD particles, which have lower stabilities. Because of the striking differences between the NRM MDF's and those of the artificial remanences, it is obvious that the ARM and IRM activate different parts of the magnetic spectrum than the residual DRM.

In contrast to the OR sediments the directions of the GC sediments, with an average within horizon angular standard deviation of 11.1°, show significantly more scatter between samples in a given horizon. Some of this variability may arise from the relatively low NRM stabilities throughout the sediment column. Overall, the core mean inclination of 41.1° (α_{95} = 2.7°,

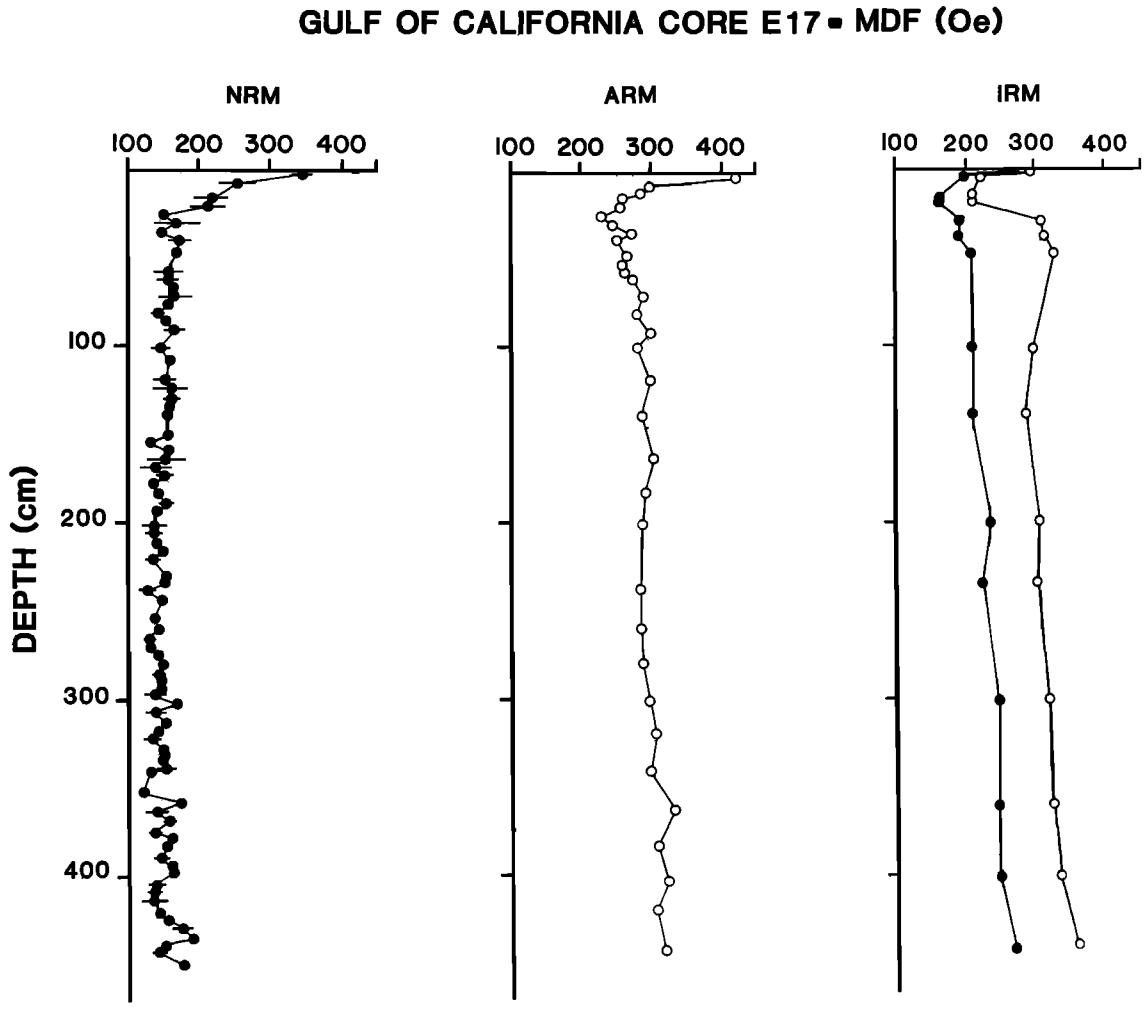

Fig. 11. Downcore profiles of NRM, ARM, and IRM MDF's. IRM's were produced at 5 kOe and ARM's at 1 kOe af with a biasing field of 0.25 Oe. Symbols are the same as in Figure 2.

k = 32.9, N = 83) compares favorably with the EGAD inclination of 46.3°, given that the core may not represent the full SV spectrum. An F test of between versus within horizon mean square variation yields a value of 1.9, which is significant at a 0.01 level. Furthermore, levels in the top 30 cm show similar within level variation as levels below the zone of reduced intensity. Thus diagenesis may not have affected the directions, and the relatively high scatter may be an artifact of the coarse-grained character of the original magnetic carriers.

Magnetic mineralogy. For the Gulf of California sediments, XRD spectra of magnetic separates from 8-12 cm and 15-21 cm show intense magnetite lines and fainter hematite lines. The sample from 197-202 cm contained magnetite but no hematite. Nonmagnetic species included quartz, opal, and plagioclase and possibly clinopyroxene, ilmenite, hypersthene, illite, and chlorite. No sulfides were positively identified, although pyrite may have been present. The magnetite unit cell parameter of 8.39 ± 0.005 A suggests that the majority of the magnetite contains little Ti in solid solution.

SEM photos of the magnetic separates from 15-21 cm (Figure 13a) show abundant siliceous debris (mostly diatoms), coarse clays, possibly hematite rhombs, and numerous agglomerates composed of diatom tests, clay booklets, and fine (<1-10 μm) magnetite euhedra. EDAX scans of the surfaces of diatom tests give Fe peaks, again suggesting surficial Fe-rich coatings. Magnetite dipyramids are well crystallized and show little evidence of mechanical abrasion or solution pitting.

Photomicrographs of the 198-202 cm separate show a coarser texture than either the top E17 samples or the OR core 28 material. Magnetite grain sizes are variable but most commonly are in the range of 1-30 μm. Many of the magnetite grains show striking evidence of surface acid etching and solution pitting (Figure 13b-13d). The extent of surface dissolution is variable, ranging from minor surface etching along fractures (Figure 13b), enhanced roughness of surface topography (Figure 13c) to deep solution pits and almost complete grain destruction (Figure 13d). Interestingly, only magnetite grains seem to have been attacked since in Figure 13b a nearby rare chromite grain shows no evidence of dissolution. IRM acquisition curves for sedi-

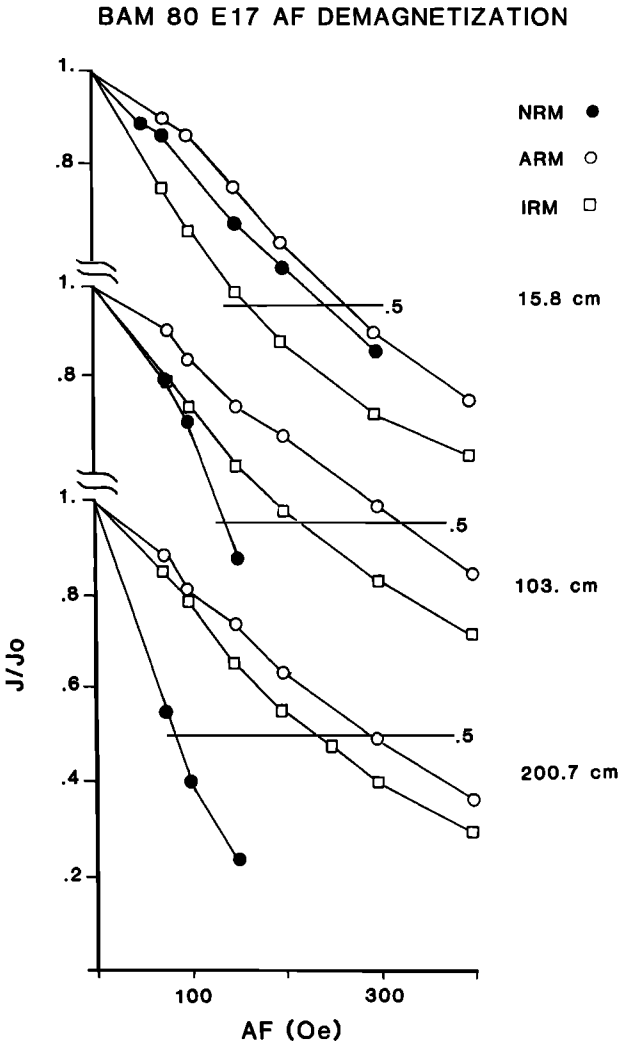

Fig. 12. Demagnetization curves of NRM, ARM, and IRM for core E17 sediments. IRM's were produced at 5 kOe and ARM's at 1 kOe af with a biasing field of 0.25 Oe. Symbols are the same as in Figure 2.

ments from core E17 (Figure 14) are consistent with a dominant magnetite component throughout the core.

X ray diffraction and Mossbauer spectroscopy. X ray diffractograms of five levels from the Gulf of California core E17 (Figure 15) gave relatively poor diffraction patterns due to high background counts and a broad hump of opal from 10° to 30° 2θ. The major diffraction peak was from quartz. Minor but recognizable reflections included pyrite, montmorillonite, illite, chlorite, and plagioclase. The diffractograms showed minor downcore variability, but owing to the poor quality of the patterns, differences could not be quantified.

Mossbauer spectra for six samples from core E17 and three clay separates were poorly resolved, probably due to low iron contents. The spectra each showed a broad central absorption area from -0.5 to 1 mm/s and a very minor secondary plateau extending to ~2.7 mm/s. For an optimal fit, constraining the heights and areas for two peak pairs was necessary. One doublet, with an average IS = 0.33 ± 0.005 mm/s, QS = 0.60 ± 0.02 mm/s, and a half width = 0.62 ± 0.09 mm/s, accounted for >80% of the total absorption area in all of the spectra. The broad line widths but narrow range of IS and QS suggest a mixture of species with one dominant component. The Mossbauer parameters are very similar to reported values for pyrite [Vaughn and Craig, 1978]; however, ferric gel can not be excluded, as noted earlier.

A second couplet, accounting for 10-17% of the total absorption, showed considerable variability between the samples' Mossbauer parameters (IS from 1.09 to 1.19 mm/s, QS from 2.36 to 2.56 mm/s, and half width from 0.33 to 0.66 mm/s). The values are within a range reported for octahedrally coordinated Fe (II) in certain amphiboles [Bancroft et al., 1968] but are too low to be associated with commonly occurring clays or pyroxenes. Verification of this identification by XRD was not possible because of the poor quality of the diffractograms.

Elemental abundances. The chemistry of the laminated diatomaceous oozes of the Guaymas Basin core E17 contrasts sharply with abundances found in the hemipelagic Oregon muds. Downcore profiles of normalized oxides (corrected for porewater Ca, Mg, S), $CaCO_3$, and organic carbon (Figure 16) as well as the statistical summary (Table 5) show a predominance of silica and large variability among the other elements. CaO values (mostly as carbonate), over 5% at the surface, decrease to about 1% below 10 cm depth. Total organic carbon decreases from over 6% at the surface to 4.7% at 10 cm, suggesting that CO_2, produced as a result of oxidative decomposition of organic matter, caused extensive carbonate dissolution in < 30 years, as determined from varve counts. Sulfate reduction can inhibit dissolution and preserve carbonate in completely anoxic waters [Dunbar and Berger, 1981]; thus the Ca, carbonate, and organic carbon curves as well as pore water sulfate [Brumsack and Gieskes, 1983] suggest that completely anoxic conditions and the onset of sulfate reduction do not begin until below 10 cm depth. This agrees with foraminifera distributions for this core [H. Schrader, personal communication, 1984]. With the exception of S and Ba, the remaining elements show substantial variability downcore but no obvious trends with depth.

Interelement correlations (upper half of Table 6) show very high correlations ($r > 0.9$) between the terrigenous elements Al, Mg, Ti, K, Mn, and Fe with slightly lower inverse correlations ($r \leq -0.8$) to Si. These associations suggest mixing between a terrigenous source, such as the nearby Rio Yaqui, and a silicous biogenic assemblage, presumably composed mostly of diatoms. The terrigenous source apparently retains a remarkably constant composition through time.

When the data are normalized to Al to remove the effects of aluminosilicates (Table 5 and lower half of Table 6), most of the variability and high correlations for Ti, Fe, and K disappear. Thus these elements must be associated with aluminosilicates, possibly as illites. However, Mg and Mn show a 0.9 correlation, and each element retains a high downcore variability

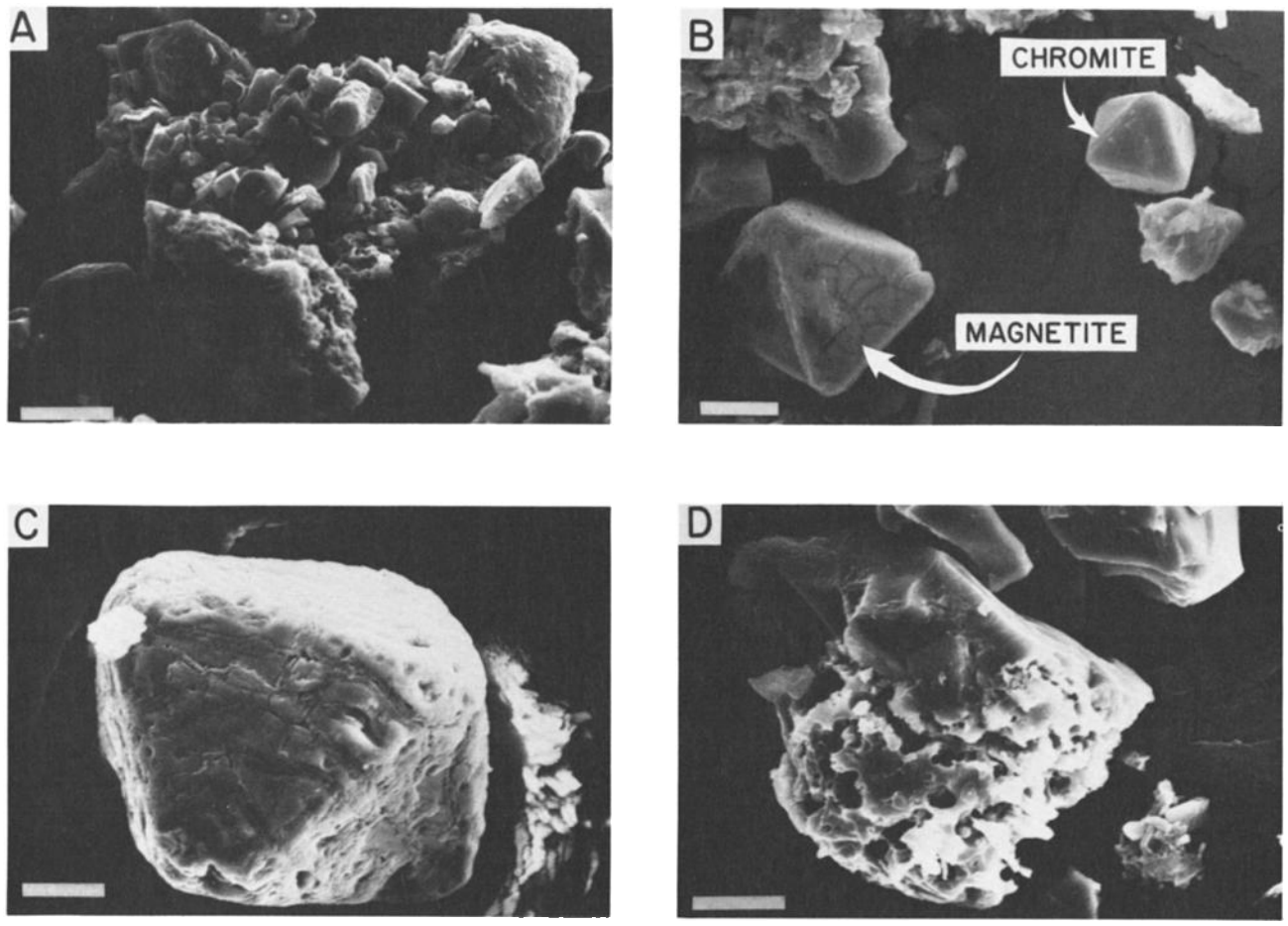

Fig. 13. SEM photomicrographs of magnetic separates from core E17. (a) For depth 15-21 cm, separates contained numerous conglomerates of clay booklets with affixed magnetite octahedra; centric and pennate diatom fragments, spores, and bristles; and plagioclase (?) rhombs. Note the mixture of grain sizes and well-crystallized octahedra. (b) For depth 198-202 cm, octahedron of magnetite (lower left) with etched surface. A nearby chromite octahedron (upper right) shows no evidence of acid attack. (c) Large (50 μm) magnetite particle showing surface etching and solution pitting indicative of acid attack. (d) Partially dissolved and deeply pitted magnetite particle. Note submicron particles attached to the surface. The scale bar is 10 μm long.

upon normalization to Al. Ca shows a moderate association with these elements, suggesting that some of the Ca, Mg, and Mn may occur in the form of rhodochrosite and/or protodolomite [Suess, 1979a]. High negative correlations with Si (0.8-0.9) might be due to dilution of these authigenic minerals by biogenic silica.

Partitioning of Iron. Using some of the same techniques as with the Oregon sediments, we can roughly partition the iron in the E17 sediments into sulfide, magnetite, and other, presumably detrital phases. Mossbauer analyses showed that only 10-15% of the total Fe was in a reduced state in noncubic minerals, such as amphiboles, pyroxenes, or phyllosilicates. For purposes of partitioning the iron, we assume that all of the sulfur is present as pyrite and that organically bound S is negligible. The Ba concentrations suggest that <2% of the sulfur could be tied up as barite. The sulfide iron estimate must be regarded as a lower limit if iron monosulfides are present.

The Fe partitioning (Figure 17) shows that sulfide iron increases in the top 60-120 cm and then fluctuates about a relatively constant value below this depth. Below 60 cm the fluctuations in pyrite iron generally covary with total iron, suggesting that the availability of reactive iron controls sulfide abundance. The proportion of pyrite iron varies from less than 20% in the top 20 cm to 55-75% throughout most of the core. These high percentages attest to the pervasiveness of diagenesis in these highly reducing sediments.

Magnetite Fe accounts for ~5% of the total iron in the topmost sediments. Abundances drop by an order of magnitude in the top 50 cm and by a factor of 30 below 220 cm. The surface magnetite Fe concentration is ~10% of the pyrite iron values at depth. Thus, as in the Oregon sediments, the magnetite iron reservoir appears to be preferentially tapped for pyrite formation.

Discussion

Possible causes for the downcore decreases in NRM intensity include fluctuations in magnetic field and changes in the mineralogy, concentra-

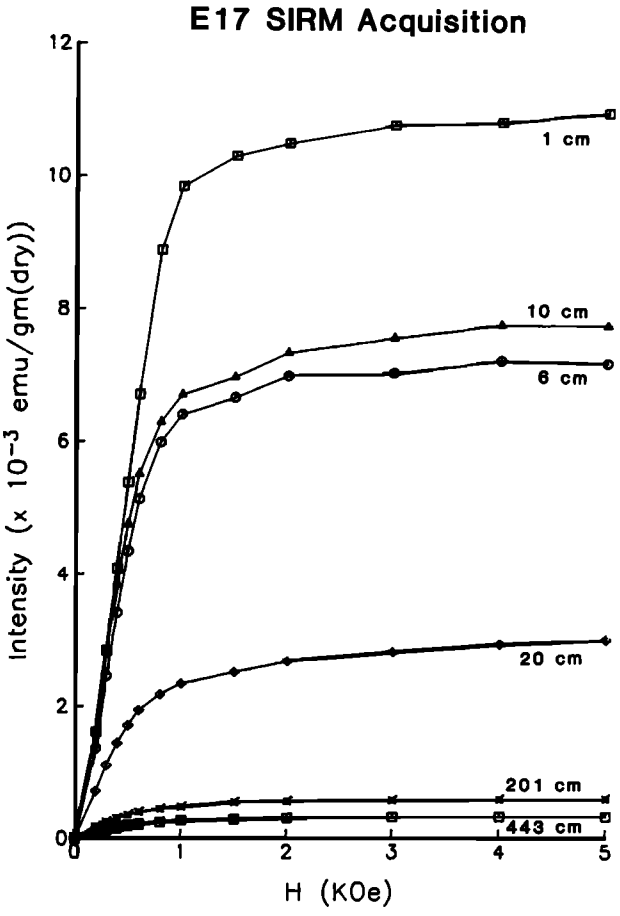

Fig. 14. Acquisition curves of saturation isothermal remanence (SIRM) for different levels of core E17.

tion, and/or size distribution of the magnetic fraction. Intensity changes in the earth's magnetic field can be discounted immediately because the downcore trends in laboratory-produced remanences parallel the NRM profiles, implying profound changes in rock magnetic properties. Fundamental differences in magnetic mineralogy with depth can also be ruled out since magnetite was the only magnetic mineral found in the magnetic separates of the Oregon cores and at depth in E17. Although hematite as well as magnetite was identified in the top 20 cm of E17, the rapid saturation of IRM at 3-5 kOe, the NRM MDF's, and the low spontaneous moment of hematite argue that the remanence in the sediments resides predominantly in magnetite.

Changes in the relative concentration and perhaps size distribution of the magnetic fraction can be due to diagenesis, authigenesis, or variations in the detrital sediment source with time. In most sediments of heterogeneous lithology, probably the most common cause of downcore fluctuations in natural and artificial remanence is due to variations in terrigenous input and detrital source mineralogy. The Oregon sediments display constant downcore profiles in major element chemistry, X ray mineralogy, and Mossbauer characteristics. Moreover, sedimentation rates are constant downcore, implying uniform detrital input with time. For the Gulf of California sediments the high covariance of terrigenous elemental abundances suggests a surprising constancy in source mineralogy with time. Accumulation rates in E17 are quite variable downcore; however, the trends in magnetic properties show no correspondence. We must then conclude that the observed trends in remanence are not caused by changes in provenance of the terrigenous material.

Unlike highly oxidized pelagic sediments where authigenic Mn-Fe hydroxides have been reported at depth in the sediment column [Henshaw and Merrill, 1980], rapidly deposited hemipelagic sediments such as found along many continental margins are typically suboxic to reducing so that oxidized authigenic minerals would not be expected. In the OR and GC sediments, authigenic Fe_3O_4 formation is unlikely, except perhaps close to the surface because in the present polarity field, authigenesis should cause a downcore increase in NRM rather than the observed decrease. Magnetic sulfides such as pyrrhotite Fe_1 S reported in the Sea of Japan [Kobayashi and Nomura, 1972] or greigite (Fe_3S_4) were not observed here. Such authigenic sulfides may require acidic conditions [Rickard, 1975] which are uncommon in marine sediments [Berner, 1981b].

The most likely cause of the downcore remanence decreases is the reduction of magnetite and subsequent formation of pyrite [Karlin and Levi, 1983]. This occurs as a result of anaerobic microbial decomposition of organic matter utilizing the ferric/ferrous transition as a source of metabolic energy. The depth where the dissolution begins is mostly a function of the amount of organic input and, secondarily, the total accumulation rate [Berner, 1981b]. In the highly reducing GC sediments the high surficial organic carbon contents (>6%) cause Fe reduction to commence in the top 10 cm, and magnetic mineral concentrations drop rapidly by a factor of 30 with depth. In the less reducing OR muds the lower carbon abundances (<3%) delay the onset of Fe reduction until ~60 cm, whereupon magnetite abundances rapidly diminish downcore by a factor of about 10.

The high NRM and ARM MDF's in the surface sediments indicate that the initial magnetic fraction is composed mainly of very fine SD and PSD particles. The NRM and ARM are also more stable than the IRM. In the transitional in-

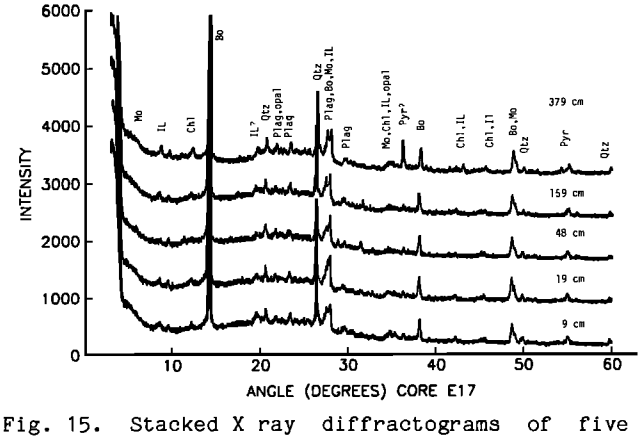

Fig. 15. Stacked X ray diffractograms of five levels from core E17. Peak identifications are the same as in Figure 6.

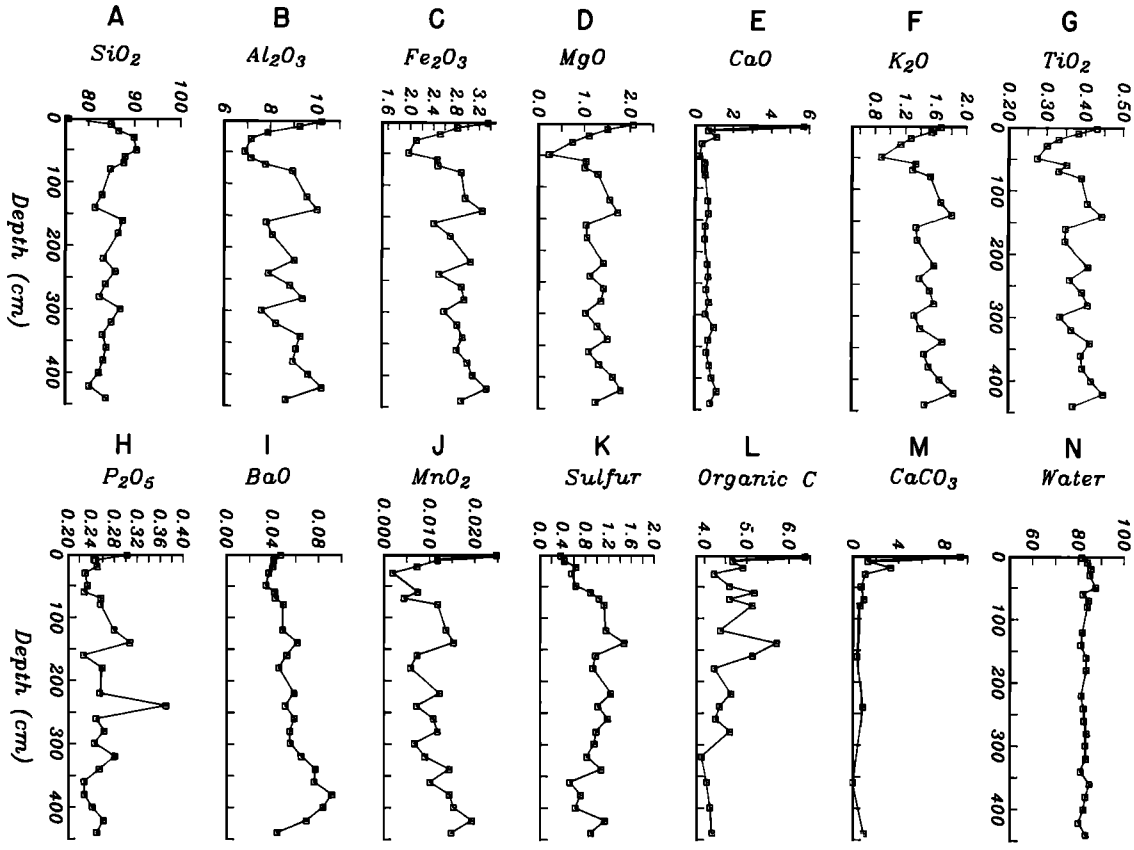

Fig. 16. Gulf of California core BAM 80 E17, downcore profiles of major element chemistry, organic carbon, $CaCO_3$, water contents, and bulk densities. Abundances, given as oxides in percent dry weight, have been corrected for seawater concentrations and are normalized so that the sum of the oxides of the 12 major elements equals 100%.

tensity zone, MDF's of all remanences drop sharply as the intensities decrease, consistent with downcore coarsening of the remaining magnetic fraction and a larger relative contribution of coarser and less stable grains. Note that the response of MDF's to particle dissolution depends on the initial particle size distribution. Because of the humped shape of the theoretical curve of relaxation time (i.e., stability) versus grain size [Merrill, 1975], it is possible that for a particular size distribution the stabilities could first increase then decrease due to progressive grain dissolution.

With depth, the MDF's of the laboratory-produced remanences increase again, although intensities remain about the same or decrease slightly. ARM stabilities show a tendency to increase relative to the IRM stabilities with depth. These trends are consistent with downcore fining of the remaining particles. NRM stabilities show no obvious corresponding trend.

The downcore increase in relative stability of ARM and IRM can be better understood by examining the SEM photos of the magnetic separates (Figures 4 and 13). The large MD sized magnetite grains show signs of extensive surface etching and solution pitting. This leads to large increases in specific surface area and formation of many small segregated regions that may behave as PSD and SD particles. Therefore, with progressive dissolution the stabilities and microscopic coercivities of the large grains would increase due to decreases in their overall

TABLE 5. Gulf of California Core E17: Summary of Chemical Analyses

	Oxide Abundances			Ratios to Al_2O_3		
Oxide	Mean	SD	%V	Mean	SD	%V
SiO_2	85.560	3.183	3.8	9.928	1.524	15.4
TiO_2	0.377	0.044	11.7	0.044	0.002	4.2
Al_2O_3	8.662	0.987	11.4	1.0	-	-
Fe_2O_3	2.783	0.355	12.8	0.321	0.015	4.7
MnO	0.011	0.006	54.5	0.001	0.0005	44.9
MgO	1.281	0.374	29.2	0.145	0.031	21.5
CaO	0.896	1.046	116.7	0.099	0.101	101.6
K_2O	1.469	0.216	14.7	0.169	0.011	6.6
P	0.258	0.032	12.4	0.030	0.004	14.9
BaO	0.055	0.015	27.3	0.006	0.001	23.1
S	0.885	0.278	31.4	0.103	0.030	29.4

See Table 3 for explanations.

TABLE 6. Gulf of California Core E17: Correlation Matrix of Oxide Abundances

	Depth	Na	Mg	Al	Si	P	K	Ca	Ti	Mn	Fe	Ba	S	Sum	H_2O	ρBulk
Depth	+	0.52	-	-	-	-	-	-	0.41	-	0.42	0.76	-	0.71	-	0.90
Na	0.53	+	0.63	0.73	-0.83	-	0.59	0.56	0.70	0.78	0.74	0.55	-	0.68	-	0.59
Mg	-	0.58	+	0.91	-0.93	-	0.95	0.56	0.93	0.94	0.94	0.45	-	-	-0.81	0.41
Al	-	-	-	+	-0.93	-	0.93	0.44	0.95	0.91	0.94	0.53	-	0.51	-0.64	0.44
Si	-	-0.86	-0.80	-	+	-	-0.86	-0.71	-0.90	-0.97	-0.94	-0.46	-	-0.47	0.67	-0.42
P	-	-0.47	-	-	0.53	+	-	-	-	-	-	-	-	-	-	-
K	-	-	0.75	-	-0.41	-	+	-	0.98	0.89	0.94	0.56	-	0.45	-0.84	0.50
Ca	-	0.48	0.50	-	-0.42	-	-	+	-	0.64	0.47	-	-	-	-	-
Ti	-	-	-	-	-	-	0.75	-	+	0.91	0.96	0.61	-	0.49	-0.80	0.52
Mn	-	0.82	0.89	-	-0.90	-0.47	0.54	0.58	-	+	0.94	0.48	-	0.50	-0.73	0.45
Fe	-	-	0.57	-	-	-	0.61	-	0.58	0.47	+	0.57	-	0.55	-0.74	0.53
Ba	0.73	-	-	-	-	-	-	-	-	-	-	+	-	0.50	-0.43	0.69
S	-	-	-	-	-	-	0.46	-0.50	0.51	-	-	-	+	-	-0.50	-
Sum	0.71	0.71	-	-	-0.54	-	-	-	-	0.53	-	-	-	+	-	0.71
H_2O	-	-0.46	-0.83	-	0.65	-	-0.85	-	-0.56	-0.74	-0.55	-	-	-	+	-0.50
ρBulk	0.90	0.59	-	-	-0.45	-	-	-	-	0.47	0.43	0.61	-	0.71	-0.50	+

See Table 4 for explanations. N = 24.

volumes and increases in SD and PSD sized regions. Because the total magnetic moment depends also on the total volume of magnetic material, no parallel increases in ARM and IRM intensities are expected.

In contrast, one would expect that the original NRM would be progressively destroyed. After initial dissolution of the finest particles the residual DRM would be carried mainly by the remaining larger grains. This would lead to an effective decrease in the "lock-in" depth and a narrower range over which remanence is fixed, since coarser particles would be locked into the matrix closer to the surface. With depth (and time) the DRM moment carried by SD and PSD grains would diminish as the initial grain surfaces are destroyed, stresses are relieved, and domain walls become unpinned. The primary effect of progressive dissolution on the NRM is in reducing its intensity. The SD/PSD regions created by dissolution pitting will generally not be carriers of NRM, so that the grains' increasing microscopic coercivities would not be reflected in the NRM stabilities.

The diagenetic processes affecting these two contrasting hemipelagic regimes influence the remanence via iron reduction and dissolution of magnetic particles, causing downcore reductions in the remanence intensities and stabilities. However, if there remain sufficient detrital magnetic grains relatively unaffected by the diagenetic dissolution and which maintain relatively high remanence stability, the paleomagnetic directions will not be degraded by this type of diagenesis, which acts primarily to remove particles from the remanence ensemble, diagenetic or dissolution demagnetization. Thus the OR sediments can be used to study detailed geomagnetic directional fluctuations. However, the GC sediments are of lesser quality for paleomagnetic studies due to the coarse grain sizes of the initial magnetic ensemble rather than diagenetic alteration.

In contrast to dissolution resistant paleomagnetic directions, relative paleointensity determinations are precluded for these diagenetically altered sediments because they fail to satisfy the requirement for the downcore homogeneity of magnetic properties [Levi and Banerjee, 1976]. This is a necessary condition for the remanence intensities to depend only on the geomagnetic field and magnetic mineral

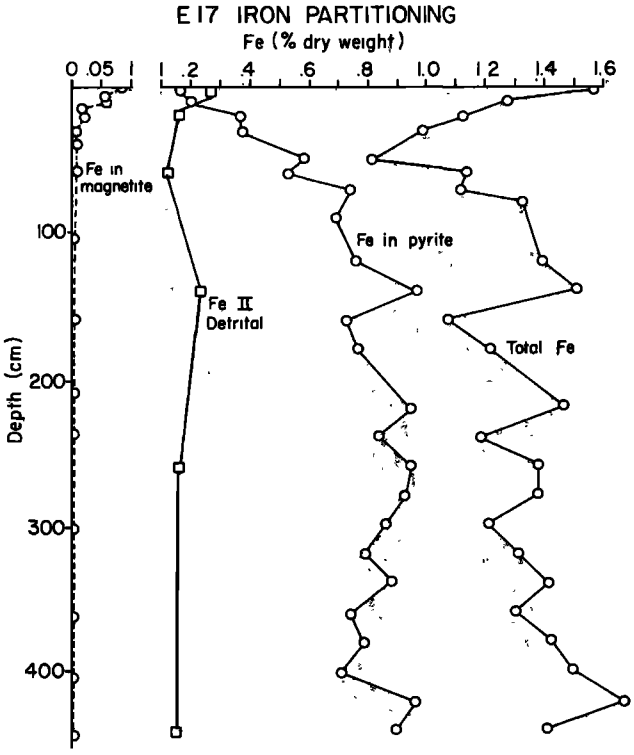

Fig. 17. Gulf of California core BAM 80 E17, partitioning of total Fe into chlorite, pyrite, magnetite, and residual phases.

concentration. Although DRM MDF's have settled to a plateau value, the progressive downcore increases of ARM and IRM MDF's suggest that diagenesis is still progressing at the bottom of the cores. Therefore relative paleointensity determinations for these sediments would provide erroneous estimates of relative geomagnetic intensities.

Although our present investigation has been restricted to suboxic and anoxic sulfidic sediments [Berner, 1981a], we would expect that other depositional regimes would be affected by early diagenesis. Ideally, organic matter decomposition reactions proceed from oxidation by O_2 to nitrate, manganese, iron, and sulfate reduction and, finally, to methanogenesis. In a given depositional regime the diagenetic sequence can be compressed, telescoped, or stopped at a certain stage depending on the availability of metabolizable organic matter and reactive oxidants.

In pelagic "red clay" regimes, very low sedimentation rates (mm/kyr) and little carbon input result in a completely oxic sediment column [Sayles and Manheim, 1975] where magnetic Fe-Mn oxyhydroxides can precipitate and magnetites can become oxidized to maghemites. In mildly reducing environments with moderate sedimentation rates (1-5 cm/kyr), authigenic magnetite may be thermodynamically stable [Henshaw and Merrill, 1980] and may be formed either as a result of partial reduction and conversion of ferric oxides or from the oxidation and reprecipitation of diagenetically remobilized porewater Fe (II) from below. This possibility has not yet been addressed.

In continental borderlands and marginal basins, iron and sulfate reduction in organic-rich, rapidly deposited (>10 cm/kyr) marine sediments causes major diagenetic alterations of magnetic minerals as iron sulfides are formed. If sulfate is absent, as in lacustrine "gyttjas" or methanic sediments, iron reduction should still occur, since iron and sulfate reduction are independent of each other [Sorensen, 1982]. Depending on the availability of bicarbonate, phosphate, and calcium, diagenetic minerals such as siderite ($FeCO_3$), vivianite ($Fe_3[PO_4]_2.8H_2O$), or protodolomite [Emerson and Widmer, 1978; Suess, 1979b; Berner, 1981a] might be diagnostic of alteration of ferrimagnetic species. Thus, in ombrotrophic peat bogs, major downcore changes in magnetic properties [Oldfield et al., 1978] might possibly be due to diagenesis rather than anthropogenic activity as they suggested. Similarly, major intensity drops in NRM, ARM, and IRM at reversal boundaries near iron-rich horizons in Miocene marine clays from Crete [Valet and Laj, 1981] may be caused by climatically induced shifts in the sediments' redox environment rather than disorientation of magnetotactic bacteria during a reversal, as proposed by Kirschvink [1982].

Conclusions

Hemipelagic sediments from contrasting sedimentation regimes are affected by similar diagenetic processes which are determined largely by high rates of sedimentation and input of organic material. In both the OR and GC sediments the oxidative decomposition of organic matter dramatically alters downcore magnetic properties. Magnetite, which is the dominant remanence carrier, is chemically reduced and progressively dissolved with depth. Initially, the smaller magnetite particles dissolve completely or to a superparamagnetic state, causing a precipitous drop downcore in the intensities of the various remanences (NRM, IRM, and ARM) accompanied by a decrease in the stabilities. Continuing farther downcore, dissolution shifts the particle size distribution to smaller grain sizes, reflected in increased stabilities of the laboratory-produced remanences at depth.

Provided enough magnetic grains survive dissolution and the remaining remanence is sufficiently stable, paleomagnetic directions can survive the diagenetic dissolution process. However, owing to diagenetically caused downcore inhomogeneities in the magnetic properties, relative paleointensity determinations are precluded for these sediments.

The recognition that magnetic minerals are strongly affected by their ambient depositional environments argues for caution in interpreting magnetic intensity results, particularly in heterogeneous lithologies. However, the sensitivity of magnetic measurements in detecting very small changes in magnetic mineral abundances opens interesting possibilities for using magnetic parameters, with other geochemical and sedimentological tools, to evaluate paleoenvironmental conditions in modern and ancient sediments.

Acknowledgments. We thank C. S. Gromme, H. Wickman, G. R. Heath, and E. Suess for use of their analytical facilities; M. Goldhaber for sulfur analyses; M. Stuiver for ^{14}C dating; and G. R. Heath, H. Schrader, and E. Suess for helpful discussions. D. Schultz provided valuable laboratory assistance. This work was partially supported by National Science Foundation grants OCE 7926440, 8310922 and a Texaco Fellowship to R. K.

References

Bancroft, G. M., Mossbauer Spectroscopy: An Introduction For Inorganic Chemists and Geochemists, 252 pp., McGraw-Hill, New York, 1973.

Bancroft, G. M., R. G. Burns, and A. J. Stone, Application of the Mossbauer effect to silicate mineralogy: Iron silicates of unknown and complex structures, Geochim. Cosmochim. Acta, 32, 547-557, 1968.

Berner, R. A., Distribution and diagenesis of sulfur in some sediments from the Gulf of California, Mar. Geol., 1, 117-140, 1964.

Berner, R. A., Principles of Chemical Sedimentology, 240 pp., McGraw-Hill, New York, 1970.

Berner, R. A., A new geochemical classification of sedimentary environments, J. Sediment. Petrol., 51, 359-365, 1981a.

Berner, R. A., Early Diagenesis: A theoretical approach, 241 pp., Princeton University Press, Princeton, N. J., 1981b.

Brindley, G. W., and G. Brown, Crystal Structures of Clay Minerals and Their X ray Identification, Monagr., vol. 5, 495 pp., Mineralogical Society, London, 1980.

Brumsack, H. J. and J. M. Gieskes, Interstitial water trace metal chemistry of laminated sediments from the Gulf of California, Mexico, Mar. Chem., 14, 89-106, 1983.

Calvert, S. E., Factors affecting distribution of laminated diatomaceous sediments in the Gulf of California, Marine Geology of the Gulf of California, edited by T. H. Van Andel and G. G. Shor, Mem. Am. Assoc. Pet. Geol., 3, 311-330, 1964.

DeMaster, D. J., The marine budgets of silica and ^{32}Si., Ph.D. thesis, 308 pp., Yale Univ., New Haven, Conn., 1979.

Dunbar, R. B., and W. H. Berger, Fecal pellet flux to modern bottom sediment of Santa Barbara Basin, California, based on sediment trapping, Geol. Soc. Am. Bull., 92, 212-216, 1981.

Duncan, J. R., Late Pleistocene and post-glacial sedimentation and stratigraphy of deep-sea environments off Oregon, Ph.D. thesis, 222 pp., Oreg. State Univ., Corvallis, 1968.

Dunlop, D. J., Magnetic mineralogy of unheated and heated red sediments by coercivity spectrum analysis, Geophys. J. R. Astr. Soc., 27, 37-55, 1972.

Emerson, S., and G. Widmer, Early diagenesis in anaerobic lake sediments, II, Thermodynamic and kinetic factors controlling the formation of iron phosphate, Geochim. Cosmochim. Acta, 42, 1307-1316, 1978.

Fisher, R. A., Dispersion on a sphere, Proc. R. Soc. London, Ser. A, 217, 295-305, 1953.

Goldhaber, M. B. and I. R. Kaplan, The sulfur cycle, in The Sea, vol. 5, edited by E. D. Goldberg, pp.569-655, John Wiley, New York, 1974.

Goldhaber, M. B. and I. R. Kaplan, Mechanisms of sulfur incorporation and isotope fractionation during early diagenesis in sediments in the Gulf of California, Mar. Chem., 9, 95-143, 1980.

Henshaw, P. C., Jr., and R. T. Merrill, Magnetic and chemical changes in marine sediments, Rev. Geophys., 18, 483-504, 1980.

Johnson, H. P., H. Kinoshita, and R. T. Merrill, Rock magnetism and paleomagnetism of some North Pacific deep-sea sediments, Geol. Soc. Am. Bull., 86, 412, 1975a.

Johnson, H. P., W. Lowrie, and D. V. Kent, Stability of anhysteretic remanent magnetization in fine and coarse magnetite and maghemite particles, Geophys. J. R. Astron. Soc., 41, 1-10, 1975b.

Karlin, R., Sediment sources and clay mineral distributions off the Oregon coast, J. Sediment. Petrol., 50, 543-560, 1980.

Karlin, R., Paleomagnetism, rock magnetism and diagenesis in hemipelagic sediments from the northeast Pacific Ocean and the Gulf of California, Ph.D. thesis, 246 pp., Oreg. State Univ., Corvallis, 1984.

Karlin, R., and S. Levi, Diagenesis of magnetic minerals in Recent haemipelagic sediments, Nature, 303, 327-330, 1983.

Kent, D. V. and W. Lowrie, Origin of magnetic instability in sediment cores from the central north Pacific, J. Geophys. Res., 79, 2987-2999, 1974.

Kirschvink, J. L., Paleomagnetic evidence for fossil biogenic magnetite in western Crete, Earth Planet Sci. Lett., 59, 388-392, 1982.

Kobayashi, K., and M. Nomura, Iron sulfides in the sediment cores from the Sea of Japan and their geophysical implications, Earth Planet Sci. Lett., 16, 200-208, 1972.

Krissek, L. K., Sources, dispersal, and contributions of fine-grained terrigenous sediments on the Oregon and Washington Continental Slope Ph.D. thesis, 174 pp., Oreg. State Univ., Corvallis, 1982.

Kulm, L. D. and K. F. Scheidegger, Quaternary sedimentation on the tectonically active Oregon continental slope, Spec. Publ. Soc. Econ. Paleontol. Mineral., 27, 247-263, 1979.

Larson, E. E., and T. R. Walker, Development of chemical remanent magnetization during the early stages of red-bed formation in late Cenozoic sediments, Baja California, Geol. Soc. Am. Bull., 86, 639-650, 1975.

Levi, S., and S. K. Banerjee, On the possibility of obtaining relative paleointensities from lake sediments, Earth Planet. Sci. Lett., 29, 219-226, 1976.

Levi, S., and R. T. Merrill, A comparison of ARM and TRM in magnetite, Earth Planet. Sci. Lett., 32, 171-184, 1976.

Levi, S., and R. T. Merrill, Properties of single-domain, pseudo-single-domain and multidomain magnetite, J. Geophys. Res., 83, 309-314, 1978.

McElhinny, M. W. and R. T. Merrill, Geomagnetic secular variation over the past 5 million years, Rev. Geophys., 13, 687-707, 1975.

Merrill, R. T., Magnetic effects associated with chemical changes in igneous rocks, Geophys. Surv., 2, 277-311, 1975.

Oldfield, F., R. Thompson, and K. E. Barber, Changing atmospheric fallout of magnetic particles recorded in Recent Ombrotrophic peat sections, Science, 199, 679-680, 1978.

Prince, R., G. R. Heath, and M. Kominz, Paleomagnetic studies of central North Pacific sediment cores: Stratigraphy, sedimentation rates, and the origin of magnetic instability, Geol. Soc. Am. Bull., 91, 1789-1835, 1980.

Rickard, D. T., Kinetics and mechanism of pyrite formation at low temperatures, Am. J. Sci., 275, 636-652, 1975.

Sayles, F. L., and F. T. Manheim, Interstitial solutions and diagenesis in deeply buried marine sediments: Results from the Deep Sea Drilling Project, Geochim. Cosmochim. Acta, 39, 103-128, 1975.

Schrader, et al., Laminated diatomaceous sediments from the Guaymas Basin slope (central Gulf of California): 250000-year climate record, Science, 207, 1207-1209, 1980.

Snedecor, G. W., and W. G. Cochran, Statistical Methods, 507 pp., Iowa State University Press, Ames, 1980.

Sorensen, J., Reduction of ferric iron in anaerobic, marine sediment and interaction with reduction of nitrate and sulfate, Appl. Environ. Microbiol., 43, 319-332, 1982.

Suess, E., Authigenic barite in varved clays, in The Dynamic Environment of the Ocean Floor, edited by K. A. Fanning and F. T. Manheim, pp. 339-355, D. C. Heath, Lexington, MA, 1979a.

Suess, E., Mineral phases formed in anoxic sediments by microbial decomposition of organic

matter, Geochim. Cosmochim. Acta, 43, 339-352, 1979b.

Suttill, R. J., P. Turner, and D. J Vaughn, The geochemistry of iron in Recent tidal-flat sediments of the Wash area, England: a mineralogical Mossbauer, and magnetic study, Geochim. Cosmochim. Acta, 46, 205-217, 1982.

Valet, J. P., and C. Laj, Paleomagnetic record of two successive Miocene geomagnetic reversals in western Crete, Earth Planet. Sci. Lett., 54, 53-63, 1981.

Van Andel, T. H., Recent marine sediments of the Gulf of California, Marine Geology of the Gulf of California, edited by T. H. Van Andel and Shor, G. G., Mem. Am. Assoc. Pet. Geol., 3, 216-310, 1964.

Vaughn, D. J., and J. R. Craig, Mineral Chemistry of Metal Sulfides, 493 pp., Cambridge University Press, Cambridge, 1978.

Verosub, K., Depositional and post-depositional processes in the magnetization of sediments, Rev. Geophys., 15, 129-143, 1977.

Watson, G. S., and E. Irving, Statistical methods in rock magnetism, Mon. Not. R. Astron. Soc. Geophys. Suppl., 7, 289-300, 1957.

Weliky, K., Clay-organic associations in marine sediments: Carbon, nitrogen, and amino acids in the fine grained fractions, M.S. thesis, 166 pp., Oreg. State Univ., Corvallis, 1982.

Wilson, R. L., Dipole offset--The time-averaged paleomagnetic field over the past 25 million years, Geophys. J. R. Astron. Soc., 22, 491-504, 1971.

R. Karlin, and S. Levi, College of Oceanography, Oregon State University, Corvallis, OR 97331.

(Received April 9, 1984;
revised April 15, 1985;
accepted April 16, 1985.)